JOURNAL OF PETROLOGY | VOLUME 46 | NUMBER 1 | PAGES 3–32 | 2005 | doi:10.1093/petrology/egh060

Magma Generation at a Large, Hyperactive Silicic Volcano (Taupo, New Zealand) Revealed by U–Th and U–Pb Systematics in Zircons

B. L. A. CHARLIER[1,2]*, C. J. N. WILSON[3], J. B. LOWENSTERN[4], S. BLAKE[2], P. W. VAN CALSTEREN[2] AND J. P. DAVIDSON[1]

[1]DEPARTMENT OF EARTH SCIENCES, UNIVERSITY OF DURHAM, SOUTH ROAD, DURHAM DH1 3LE, UK

[2]DEPARTMENT OF EARTH SCIENCES, THE OPEN UNIVERSITY, WALTON HALL, MILTON KEYNES MK7 6AA, UK

[3]INSTITUTE OF GEOLOGICAL & NUCLEAR SCIENCES, PO BOX 30368, LOWER HUTT 6315, NEW ZEALAND

[4]VOLCANO HAZARDS TEAM, US GEOLOGICAL SURVEY, MAILSTOP 910, 345 MIDDLEFIELD ROAD, MENLO PARK, CA 94025, USA

RECEIVED SEPTEMBER 25, 2003; ACCEPTED JULY 15, 2004
ADVANCE ACCESS PUBLICATION SEPTEMBER 9, 2004

Young (<~65 ka) explosive silicic volcanism at Taupo volcano, New Zealand, has involved the development and evacuation of several crustal magmatic systems. Up to and including the 26·5 ka 530 km^3 Oruanui eruption, magmatic systems were contemporaneous but geographically separated. Subsequently they have been separated in time and have vented from geographically overlapping areas. Single-crystal (secondary ionization mass spectrometry) and multiple-crystal (thermal ionization mass spectrometry) zircon model-age data are presented from nine representative eruption deposits from ~45 to ~3·5 ka. Zircon yields vary by three orders of magnitude, correlating with the degrees of zircon saturation in the magmas, and influencing the spectra of model ages. Two adjacent magma systems active up to 26·5 ka show wholly contrasting model-age spectra. The smaller system shows a simple unimodal distribution. The larger system, using data from three eruptions, shows bimodal model-age spectra. An older ~100 ka peak is interpreted to represent zircons (antecrysts) derived from older silicic mush or plutonic rocks, and a younger peak to represent zircons (phenocrysts) that grew in the magma body immediately prior to eruption. Post-26·5 ka magma batches show contrasting age spectra, consistent with a mixture of antecrysts, phenocrysts and, in two examples, xenocrysts from Quaternary plutonic and Mesozoic–Palaeozoic metasedimentary rocks. The model-age spectra, coupled with zircon-dissolution modelling, highlight contrasts between short-term silicic magma generation at Taupo, by bulk remobilization of crystal mush and assimilation of metasediment and/or silicic plutonic basement rocks, and the longer-term processes of fractionation from crustally contaminated mafic melts. Contrasts between adjacent or successive magma systems are attributed to differences in positions of the source and root zones within contrasting domains in the quartzo-feldspathic (<15 km deep) crust below the volcano.

KEY WORDS: *zircon; U-series dating; rhyolite; Taupo Volcanic Zone; Taupo volcano*

INTRODUCTION

Silicic magmatism

Silicic magmatism encompasses a range of processes and products that are important in understanding the origins and differentiation of continental crust, the generation of ore deposits, and the frequency and dynamics of large explosive eruptions. Although virtually all large-scale silicic magmatism ultimately derives its thermal energy from mantle-derived mafic magmas (e.g. Hildreth, 1981), a major challenge is to unravel the mechanisms and timings whereby silicic magmas (especially rhyolites) are generated and stored prior to eruption.

*Corresponding author. Present address: Department of Earth Sciences, The Open University, Walton Hall, Milton Keynes MK7 6AA, UK. Telephone: +44(0)1908 652558. Fax: +44(0)1908 655151. E-mail: b.l.a.charlier@open.ac.uk

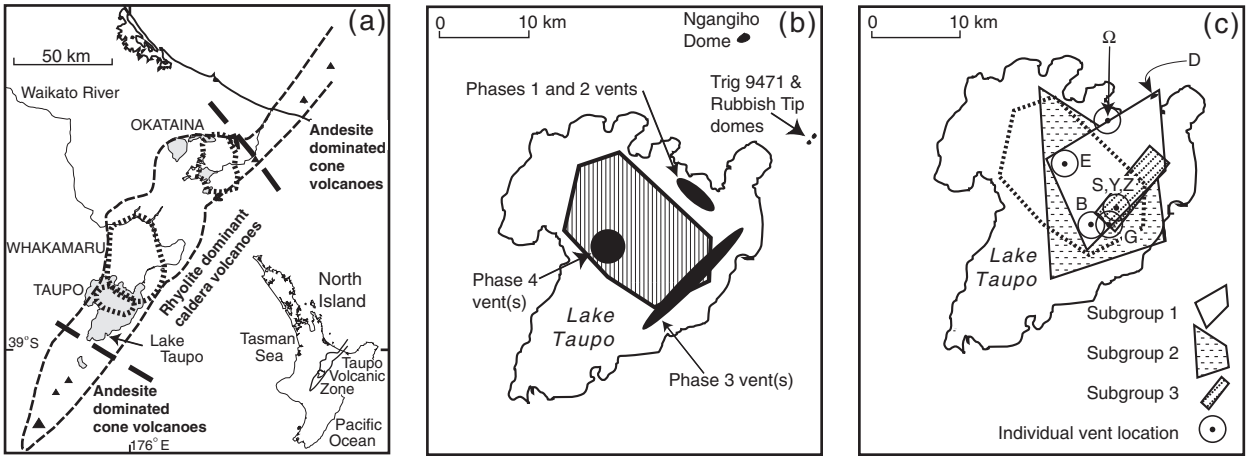

Fig. 1. (a) Location of Taupo and Okataina volcanoes, and the slightly older Whakamaru caldera, within the Taupo Volcanic Zone in the North Island of New Zealand. (b) Map of Taupo, showing vent areas for the Rubbish Tip, Trig 9471 and Ngangiho domes ['NE dome' magma type of Sutton *et al.* (1995)], the first four phases of the 26·5 ka Oruanui eruption (Wilson, 2001) and the structural core of the Oruanui caldera (shaded trapezium). (c) Map of envelopes around vent sites for eruptions representing the three post-Oruanui rhyolite magma subgroups (Sutton *et al.*, 2000), for eruptions B to E (subgroup 1), F to W (subgroup 2), and X to Z (subgroup 3), respectively (modified after Wilson, 1993). Vent sites for the individual post-Oruanui eruptives sampled [i.e. Ω, B, Acacia Bay dome (D), E, G, S and Y] are marked. Dotted line represents the Oruanui structural caldera.

In general, there is continuing debate about three key aspects of crustal magmatic systems.

(1) The roles of two possible end-member origins for the silicic magmas: first, the fractionation of silicic melts from mafic mantle-derived magmas, or second, the remelting of sedimentary or igneous crustal protoliths. Between these end-members, silicic magmatism may represent growth of wholly new crust or the recycling or remobilization of existing crustal material. Proportions of 'new' vs 'recycled' material can be delimited using isotopic evidence (e.g. Halliday *et al.*, 1984; Hildreth *et al.*, 1991; Wark, 1991; Davies *et al.*, 1994; McCulloch *et al.*, 1994; Graham *et al.*, 1995) provided that the isotopic characteristics of any pre-existing crustal materials are known and that there is a contrast.

(2) The timing of development of large silicic magma bodies, that feed eruptions of 10^1–10^3 km^3 and are accompanied by caldera collapse. There are two contrasting overall models. The first treats the growth of such magma bodies as gradual, requiring on average $\sim 10^3$ yr/km^3 of erupted magma (Smith, 1979; Spera & Crisp, 1981; Shaw, 1985; Jellinek & DePaolo, 2003). The second proposes that silicic magmas can be generated rapidly by fusion of crustal lithologies by mantle-derived melts (e.g. Huppert & Sparks, 1988*a*; Bergantz, 1989).

(3) The nature of large silicic magmatic systems prior to and during eruptions. Smith (1979) and Shaw (1985), for example, proposed that such systems are long-lived entities from which, in any one eruption, at most ~10% of the magma is discharged. Thus at any stage, large quantities of magma are potentially available to erupt and the system's petrological and thermal evolution is buffered by the un-erupted, volumetrically dominant portion of magma. In contrast, in its most extreme form, the model of Huppert & Sparks (1988*a*) generates magma bodies that exist for only short periods ($<\sim 10^3$ years), because of their limited thermal capacity, before they become >50% crystallized (and effectively immobile). Thus any magma chamber is transient and for long periods of time no significant body of magma need exist. Between these two extremes, a rich variety of possible thermal and magmatic scenarios exists (e.g. Hildreth, 1981; Annen & Sparks, 2002).

Quantifying these three aspects is important in understanding of the genesis of silicic volcanic rocks, and reconstructing their parental magma systems. In this paper we use U–Th and U–Pb isotopic systematics in zircons from eruptive units at Taupo, New Zealand, to address the nature of magma generation and storage at an exceptionally frequently active and productive silicic volcano. Together with published evidence on the timing, and geochemical and bulk isotopic variations of these eruptives, we use these age data to model the nature and evolution of magmatic systems below Taupo over the past ~65 kyr.

Taupo volcano

Taupo is one of two (along with Okataina) highly active silicic volcanoes in the central, rhyolite caldera-dominated segment of the Taupo Volcanic Zone (TVZ) in New Zealand (Fig. 1a). The TVZ has been active for

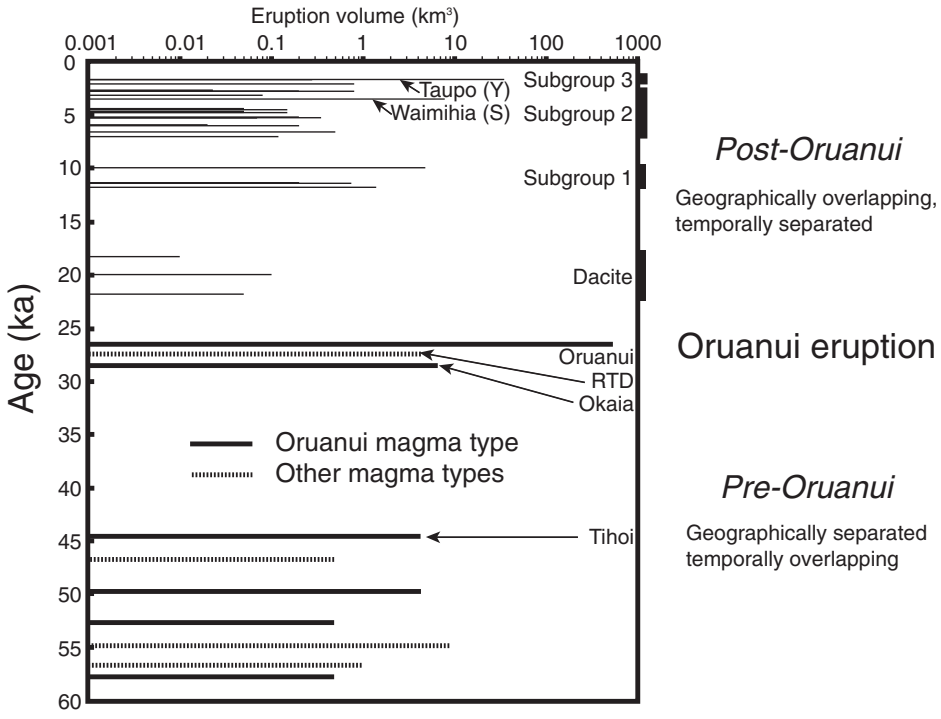

Fig. 2. Plot of age vs eruption volume for post ~60 ka eruptives from Taupo volcano. Volumes plotted for the Oruanui, Waimihia (S) and Taupo (Y) are magma volumes, including intracaldera fill in the first and last of these. Others are minimum bulk volumes based on isopach data (Wilson, 1993). RTD, Rubbish Tip dome. (See text for discussion.)

~2 Myr, with early andesitic volcanism joined from ~1·6 Ma by large-scale silicic volcanism (see Graham *et al.*, 1995; Houghton *et al.*, 1995; Wilson *et al.*, 1995, for reviews). Existing studies at Taupo volcano have established a partial eruptive chronostratigraphy (Vucetich & Howorth, 1976; Wilson, 1993, and unpublished data, 2004), together with a geochemical and isotopic database (Sutton, 1995; Sutton *et al.*, 1995, 2000; Charlier, 2000) (Fig. 2). The ~300 kyr eruption record at Taupo is dominated by the climactic ~530 km^3 (magma), 26·5 ka Oruanui eruption (Wilson, 2001; Wilson *et al.*, in preparation). For ~40 kyr prior to the Oruanui eruption, there were several distinct rhyolite compositions erupted at Taupo (Wilson *et al.*, 2002) (Fig. 3), but vents for these were geographically separated (e.g. Fig. 1b). In contrast, post-Oruanui eruptives show no geochemical, isotopic or mineralogical linkages to the climactic event (e.g. Fig. 3), and are grouped into one dacite and three rhyolite magma batches (Sutton *et al.*, 2000). These batches and their inferred magmatic systems are separated in time but have vented over geographically overlapping areas (Fig. 1c).

Taupo is an excellent case study with which to test competing models for the dynamics and evolution of youthful large silicic magmatic systems. Erupted volumes (~580 km^3 in the past 65 kyr) are similar to those of archetypal caldera-related systems such as Long Valley and Valles, and eruption rates are similar to those of Yellowstone, permitting realistic comparisons. However, the eruption frequency at Taupo is unusually high; instead of single 'snapshots' at intervals of 10^4–10^5 years (see Smith, 1979) of a magma system of this size, a 'strobe-light' effect is given by eruption frequencies often of $<10^2$–10^3 years (Wilson, 1993; Sutton *et al.*, 2000).

In this paper we present zircon geochronology data from nine eruptive units, from ~45 to 3·6 kyr old, that represent most of the magma types or batches erupted during the lead-up to the Oruanui event, the Oruanui event itself, and the younger, post-Oruanui dacitic and rhyolitic eruptions (Table 1). The main omission is the youngest (<2·1 ka) rhyolite batch, where sampling of the most voluminous deposits (Unit Y, 1·8 ka) has failed to yield any zircons. All samples are represented by U–Th thermal ionization mass spectrometry (TIMS) data (some with analyses from different size fractions), with representative examples (where sufficient zircon was available) also being analysed by secondary ionization mass spectrometry (SIMS). TIMS methods yield high precision, and are useful for obtaining the best 'average' age for the zircon population. In contrast, SIMS methods yield unique information about the spectrum of individual crystal ages and/or periods of crystal growth, albeit with lower precision. Individual grains were initially

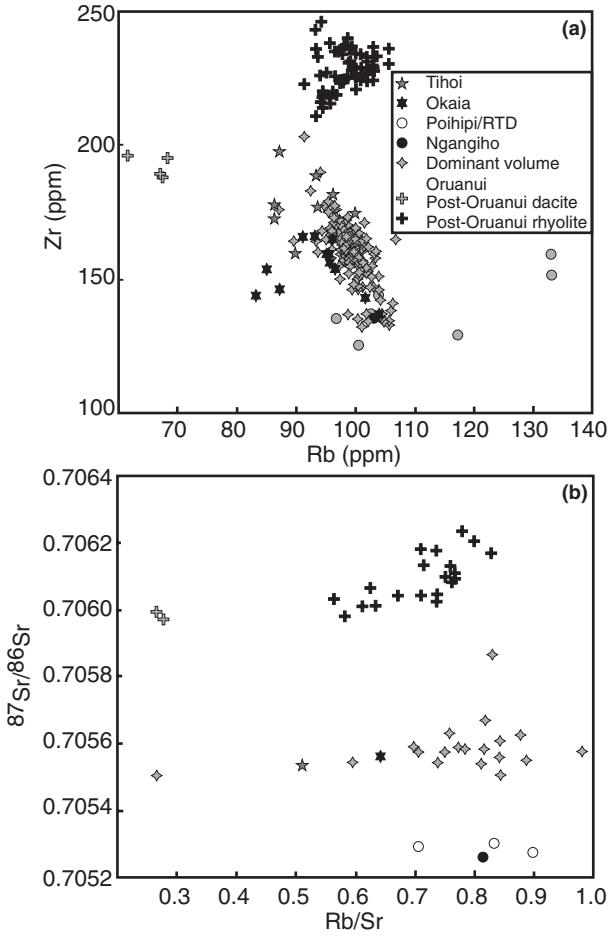

Fig. 3. Plots of (a) Zr vs Rb and (b) $^{87}Sr/^{86}Sr$ vs Rb/Sr to illustrate some compositional variations that discriminate the Poihipi–Rubbish Tip dome (RTD), Oruanui and post-Oruanui magmatic systems. Data from Sutton (1995), Sutton *et al.* (1995, 2000) and B. L. A. Charlier (unpublished data, 2000).

analysed for U-series disequilibrium and, for two samples (Units Ω and G) where there were numerous grains yielding ages close to or on the equiline, then reanalysed for U–Pb. Our main approach in U–Th dating is to use zircon separates along with host whole-rock values to define two-point isochrons.

ANALYTICAL METHODS

Samples for zircon separation consisted of single pumices, multiple pumices, or blocks of pumiceous dome carapace (Table 1). Each sample was crushed initially to pass a 710 μm mesh, then sieved into >250 μm, 250–125 μm, 125–63 μm, and <63 μm fractions. All material >250 μm was then crushed again to pass the 250 μm mesh. Preconcentration of heavy minerals was achieved within each size fraction by using water fluidization to induce density segregation between the minerals and glass (Charlier, 2000). Any remaining glass and light-mineral phases were subsequently removed from the preconcentrated dense fractions using heavy liquids, and zircon was concentrated by magnetic separation. The concentrates were placed in 3N HF and HCl for 20 min to remove adhering glass, then hand-picked as a final purification step and to remove damaged crystals. In principle, three size fractions of zircon were thus prepared, but in practice zircon yields varied by a factor of $\sim 10^3$ (Table 2) and in some cases size fractions were combined to provide sufficient material for analysis.

For TIMS analysis, ~1 mg of each zircon size fraction was weighed to ±0·1 μg, then dissolved separately in steel-jacketed Teflon® bombs. Additionally, for analysis of each whole rock, and the main mineral phases in sample Oruanui 1 (orthopyroxene, hornblende, plagioclase and magnetite), 0·1–1 g was used. Samples were checked for complete dissolution using a binocular microscope. Th and U concentrations (determined using a mixed ^{229}Th–^{236}U tracer) and Th and U isotope ratios were analysed by TIMS at The Open University using a Finnegan MAT 262 fitted with an RPQ-II energy filter (van Calsteren & Schweiters, 1995). Chemical procedures and sample loading methods used have been described by Turner *et al.* (1996). Analytical details, including estimates of precision and blanks, are given in the footnotes to Electronic Appendix 1, which contains all the TIMS results. Electronic appendices may be downloaded from the *Journal of Petrology* website at http://www.petrology.oupjournals.org.

SIMS U–Th and U–Pb analyses were carried out using the SHRIMP-RG instrument at the joint USGS–Stanford University facility and the U–Th techniques used were similar to those of Lowenstern *et al.* (2000). Zircons from eight samples were mounted in epoxy resin, polished, photographed in reflected light, and imaged by cathodoluminescence (CL). The mount was acid rinsed, coated with 100 nm of Au and left in the SHRIMP-RG sample chamber overnight to reach full vacuum. Using a 56 nA $^{16}O^-$ or $^{16}O_2^-$ primary ion beam, a 50 μm × 37 μm rectangular region was rastered for 2 min to remove the Au coat and any surface contamination. A flat-floored elliptical pit 2 μm × 25 μm × 37 μm was then excavated into the zircon. This liberated ~4–6 ng of sample that was sent as positive secondary ions to the mass spectrometer. Data were collected in 10 scans per point for $^{90}Zr_2{}^{16}O$, $^{230}Th^{16}O$, ^{232}Th, $^{232}Th^{16}O$, ^{238}U and $^{238}U^{16}O$. Scan times ranged from 2 to 15 s for each peak.

A U–Th fractionation factor was empirically determined for each 24 h period of analysis through the repeated analysis of three zircon standards: AS57 (concentration standard), from the 1·1 Ga Duluth Complex, Minnesota (Paces & Miller, 1993); SR878, from a 490 ka

Table 1: Listing of samples and techniques used

Eruption unit	Age (ka)	Sample label	Grid reference	Material sampled	TIMS	SIMS U/Th	SIMS U/Pb
Tihoi	~45	P433	T17/619829	multiple pumices	X	X	—
Okaia	29	97/P1195	U18/737785	multiple pumices	X	X	—
Poihipi/Rubbish Tip dome	27·3	97/R559	U18/818750	pumiceous glassy lava	X	X	—
Oruanui 1	26·5	P1209	U19/748448	single pumice	X	—	—
Oruanui 2	26·5	P1373	T17/501052	single pumice	X	X	—
Oruanui 3	26·5	P1520	U19/710461	single pumice	X	X	—
Unit Ω	20·0	97/P1106	U18/708741	multiple pumices	X	X	X
Unit B	11·8	97/P1157	U19/662525	multiple pumices	X	X	—
Unit D/Acacia Bay dome	11·4	97/R677	U18/735737	pumiceous glassy lava	X	—	—
Unit E	10·0	97/P1144	U18/916714	multiple pumices	X	—	—
Unit G	6·7	97/P1158	T18/657506	multiple pumices	X	X	X
Unit S	3·6	97/P471	U18/900580	multiple pumices	X	—	—

Eruption unit names and ages from Wilson (1993, and unpublished data, 2000) and Vucetich & Howorth (1976), modified for Okaia, Poihipi and Unit Ω by a new compilation of ages given by Newnham *et al*. (2003). Grid references are represented by the sheet number and 100 m grid reference in the New Zealand metric map grid. For the Poihipi and Unit D eruptions, the material analysed was collected from the co-eruptive lava dome listed. For the Oruanui, three large pumices from coarse Phase 10 ignimbrite (Wilson, 2001) were analysed separately. Unit Ω is dacite; all others are rhyolite. X, data presented in this paper; —, not analysed.

Table 2: Summary of approximate zircon yields from samples

Sample	Age (ka)	Amount crushed (kg)	Mass of zircon (mg)	Concentration (mg/kg)
Tihoi	~45	12	9·6	0·8
Okaia	29	9·3	8·6	0·9
Poihipi/RTD	27·3	12·3	6·18	0·5
Oruanui 2	26·5	2·8	2·56	0·9
Oruanui 1	26·5	5	4·68	0·9
Oruanui 3	26·5	9·5	7·56	0·8
Unit Ω	20	18	0·04	0·0022
Unit B	11·8	7·2	8·9	1·2
Unit D/ABD	11·4	7·2	3·2	0·4
Unit E	10	5·1	5·7	1·1
Unit G	6·7	25·4	4·9	0·2
Unit S	3·6	11·7	0·4	0·03
Unit Y	1·8	15	0	0

RTD, Rubbish Tip dome; ABD, Acacia Bay dome. Ages from Newnham *et al*. (2003) (Okaia, RTD), and Wilson (1993). Age for Unit Ω modified from Wilson (1993) in the light of revised ages for bracketing tephras presented by Newnham *et al*. (2003).

dioritic plutonic xenolith from Mt. Rainier (Stockstill *et al.*, 2002); R33, from a quartz diorite of the Braintree Complex, Vermont. An age of 419 Ma for the last has been established by conventional U–Pb TIMS analyses on single- and multi-grain samples by R. Mundil and S. L. Kamo at the Royal Ontario Museum, Toronto (J. Aleinikoff, personal communication, 2003). ^{238}U and ^{230}Th activities in these zircons are at secular equilibrium and therefore, after the application of a U–Th fractionation factor, the calculated activity of ($^{230}Th/^{238}U$) should equal unity. This was determined on a daily basis using the measured $^{230}Th^{16}O^{+}/^{238}U^{16}O^{+}$ ratios. To achieve a weighted mean ($^{230}Th/^{238}U$) of unity for the standards, fractionation factors varied between 1·01 and 1·09 over the analysis period, the reciprocals of which were applied in the calculation of the ($^{238}U/^{232}Th$) of the Taupo zircons for the relevant day of their analysis.

A difference between procedures applied in earlier work (e.g. Reid *et al.*, 1997; Lowenstern *et al.*, 2000; Charlier *et al.*, 2003*b*) and those used here is in the treatment of errors associated with determinations of the U/Th fractionation factor. Values of the factor varied between successive determinations, in addition to errors associated with the individual determinations that were used to regress for the fractionation factors themselves. For this paper, we recorded variations in the U/Th values for standards runs to arrive at a conservative best-estimate 1σ error of ±3% on the fractionation factor, which translates into a corresponding ±3% error on the ($^{238}U/^{232}Th$) values. This error is substantially larger than the errors calculable from the count statistics alone and hence is inferred to give a more robust limit to total errors in the ($^{238}U/^{232}Th$) values. Incorporation of this error value does not change the model ages over those calculated by previous techniques, but increases the size

of the errors on the model age by a factor varying by ~1% for an age of 50 ka to ~10% for an age of 200 ka. ^{230}Th–^{238}U isochron ages were calculated as two-point model ages by referencing each of the zircon analyses in turn to the respective whole-rock analyses. In this study, the zircons are considered to have the same initial ($^{230}Th/^{232}Th$) as the host rocks, and as the initial ($^{230}Th/^{238}U$) of the zircons are so low, calculated Th isotope ages are relatively insensitive to variations in the initial ($^{230}Th/^{232}Th$). In addition, the lack of calculated ages that are younger than eruption ages also suggests that model ages can be considered meaningful. The full SIMS U–Th dataset is presented in Electronic Appendix 2.

For SIMS U–Pb analyses in the SHRIMP-RG, techniques used were similar to those of Dalrymple *et al.* (1999). Ions were sputtered from zircons with a 10·5 nA primary O_2^- beam focused to a 25 μm × 35 μm spot. To minimize contamination by common Pb, the grain mount was cleaned in 1N HCl acid for 5 min and the primary beam was rastered for 240 s on a 150 μm^2 area prior to data acquisition. The mass spectrometer was cycled eight times through peaks corresponding to $^{90}Zr_2{}^{16}O$, ^{204}Pb, background, ^{206}Pb, ^{207}Pb, ^{208}Pb, ^{238}U, $^{232}Th^{16}O$ and $^{238}U^{16}O$. Because the zircon/melt partition coefficient is higher for U than for Th, an initial deficit of ^{230}Th may occur in zircon during its crystallization creating a temporal gap in the $^{230}Th/^{234}U$ secular equilibrium of the ^{238}U decay chain and hence an underestimation of the true age of zircon crystallization. Using the observed magnitude of zircon Th/U fractionation [$f = (Th/U_{zir})/(Th/U_{magma})$] derived from an average of the isotope dilution concentration measurements of zircons analysed by TIMS, a correction was applied using the method of Schärer (1984). The age correction resulting from initial Th–U disequilibria was in the range +0·04 to +0·11 Ma. The full U–Pb dataset is presented in Electronic Appendix 3.

RESULTS

Tihoi

The Tihoi was a moderate-sized explosive eruption, approximately dated from palaeosol development with respect to dated marker horizons at ~45 ka (C. J. N. Wilson, unpublished data, 2004). Its chemical and isotopic characteristics closely resemble those of the later Okaia and Oruanui rhyolites (Fig. 3), and it has been inferred to be derived from the same source (Sutton *et al.*, 1995). The vent position is not accurately located, but lies within the northern part of Lake Taupo (Vucetich & Howorth, 1976; C. J. N. Wilson, unpublished data, 2004), within the area encompassed by the Oruanui caldera collapse.

TIMS data

Three bulk zircon aliquots were analysed, along with a whole-rock sample. Two-point isochrons derived from these data yield model ages of 75·9 ± 1·5, 66·4 ± 1·0 and 63·5 ± 1·4 ka (Fig. 4a).

SIMS data

Forty data points gave meaningful ages in the U–Th system. These data are presented as an equiline plot for comparison with the TIMS data in Fig. 4b, and as rank plots and age histograms, with a probability distribution function (PDF) curve fitted using Isoplot (Ludwig, 2002) in Fig. 4c. There are two peaks in the model-age spectrum. One is weakly defined, centred on 61 ka, and is interpreted to represent zircons that were actively growing at the time of eruption. The other at 104 ka represents an older population.

Okaia

The Okaia fall deposit represents the last precursor eruption with similar chemical and isotopic characteristics to the Oruanui eruption (Fig. 3). Like the Tihoi, the vent position is not accurately located, but it also lies within the Oruanui caldera collapse area. Radiocarbon ages bracketing Okaia fall deposits imply a calendar age of 29 ka (Newnham *et al.*, 2003).

TIMS data

Six zircon aliquots were analysed, along with a whole-rock sample. Two aliquots were of <63 μm fractions, and the others were from 63–250 μm material. Any preferential growth of younger zircons should cause a bias towards younger ages in the smaller size fractions (compare Oruanui: Charlier & Zellmer, 2000), but there are no systematic relationships between crystal size and age in the Okaia. The model ages vary from 47 to 69 ka (Fig. 5a).

SIMS data

Twenty-six data points gave meaningful ages (Fig. 5b and c). As in the Tihoi, there is a bimodal distribution of model ages, with maxima in the PDF curve at 27 ka and 95 ka. The older peak is, within the 1σ errors associated with the individual model ages, the same as its counterparts in the Tihoi and Oruanui samples. The younger peak is interpreted as representing zircons that were crystallizing at the time of the eruption. It should be noted that there are no Okaia zircons with model ages the same as that of the Tihoi eruption (Fig. 4c), showing that the Tihoi eruption did not affect crystallization in the Okaia magma.

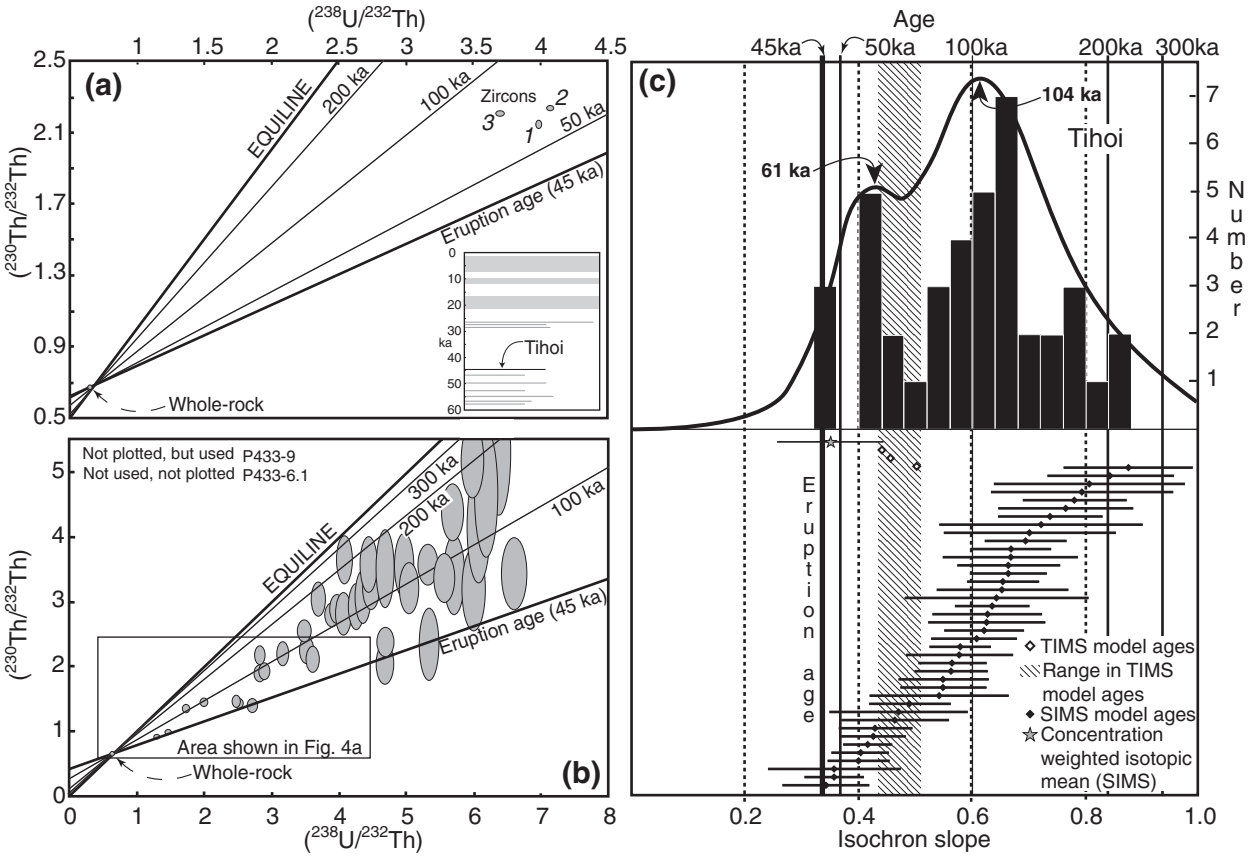

Fig. 4. Data from the Tihoi samples. (a) TIMS (^{230}Th/^{232}Th) vs (^{238}U/^{232}Th) equiline diagram for bulk zircon and whole-rock analyses. Error ellipses represent 2σ analytical uncertainties. Model ages: 1, 63·5 ± 1·4 ka; 2, 66·4 ± 1·0 ka; 3, 75·9 ± 1·5 ka; 2σ errors. Reference isochrons indicate the eruption age (~45 ka), 50 ka and subsequent 100 ka increments. Inset in this and subsequent equiline diagrams shows the highlighted stratigraphic position of the relevant eruption, from Fig. 2. Analytical data are presented in Electronic Appendix 1. (b) SIMS (^{230}Th/^{232}Th) vs (^{238}U/^{232}Th) equiline diagram for single zircons. Error ellipses represent 1σ analytical uncertainties on (^{230}Th/^{232}Th) and a standard 3% error on (^{238}U/^{232}Th) (see text for details). Reference isochrons are as in (a). Points lying within error of the equiline are not used in the construction of the probability density function (c), and points not plotted but used lie outside the plot area and are omitted for the sake of scale. Model ages and analytical data are given in Electronic Appendix 2. (c) Rank order plot (bottom) and cumulative probability density function (PDF) curve and histogram (top) based on isochron slopes derived from two-point whole-rock–zircon SIMS determinations from (b). For the rank plot, each data point shows the 1σ error bar (symmetrical with respect to the slope value). Eruption age is marked, and the TIMS bulk zircon ages and their range (shaded) are included for comparison (errors smaller than symbol size unless shown). A concentration-weighted isotopic mean age was determined by weighting all the SIMS (^{230}Th/^{232}Th) and (^{238}U/^{232}Th) values according to the U and Th concentrations of each analysis (to nearest 100 ppm; see Electronic Appendix 2). An isochron slope and age was determined by referencing this isotopic average data point to the whole rock to generate a two-point model age (error shown at the 2σ level). For the histogram, a PDF line, generated using the cumulative probability function in Isoplot (Ludwig, 2002), is superimposed and annotated with the ages of the two peaks in probability.

Poihipi (Rubbish Tip dome)

A widespread fall deposit, the Poihipi Tephra (Vucetich & Howorth, 1976) with a calendar age of 27·3 ka (Newnham *et al.*, 2003), is correlated on stratigraphic and geochemical grounds with two domes, one at Trig 9471 and the other temporarily exposed in and named after the Taupo Township rubbish tip (Fig. 1; Sutton *et al.*, 1995; Wilson *et al.*, 2002). Although occurring between the Okaia and Oruanui eruptions, the Poihipi is distinctly different in composition (Fig. 3). Material was collected from the pumiceous carapace to the Rubbish Tip dome (Sutton, 1995) because the fall deposit is very fine grained and contaminated by abundant lithics from a nearby older lava.

TIMS data

Four aliquots of 63–125 μm material were analysed, together with a whole-rock sample. Larger zircons (125–250 μm) were too scarce for TIMS work (although utilized for SIMS analysis), and smaller zircons were not found. The samples yield two-point isochron model ages between 40·1 ± 0·6 ka and 51·6 ± 0·8 ka (Fig. 6a), broadly comparable with those found in the immediately preceding Okaia eruption deposits.

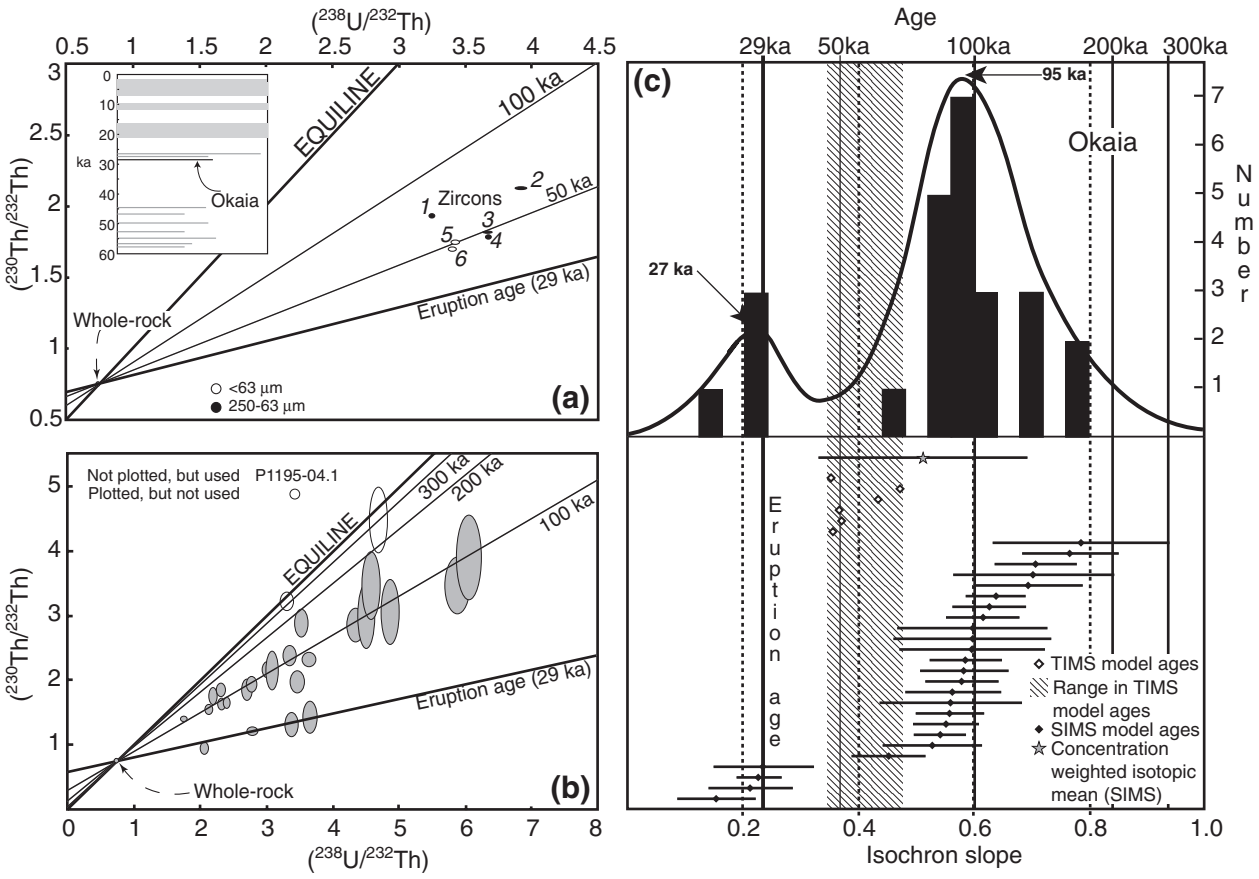

Fig. 5. Data from the Okaia samples. (a) TIMS ($^{230}Th/^{232}Th$) vs ($^{238}U/^{232}Th$) equiline diagram for bulk zircons and whole rock. Model ages: 1, 69·3 ± 1·1 ka; 2, 61·9 ± 1·4 ka; 3, 49·6 ± 0·9 ka; 4, 47·3 ± 1·2 ka; 5, 50·4 ± 1·3 ka; 6, 47·9 ± 1·3 ka; 2σ errors. (b) SIMS ($^{230}Th/^{232}Th$) vs ($^{238}U/^{232}Th$) equiline diagram for single zircons. Analyses within error of the equiline plotted as open ellipses. (c) Rank order plot (bottom) and cumulative probability density curve and histogram (top) from SIMS data. Other details as in Fig. 4.

SIMS data

Twenty-one data points were obtained (Fig. 6b and c). The model-age spectrum for the Rubbish Tip Dome sample differs markedly from those of the Tihoi, Okaia and Oruanui samples. The model ages form a unimodal distribution, with a PDF peak at 54 ka, similar to the four model ages obtained from TIMS analysis. In addition, the oldest individual model age obtained is 88 +19/–16 ka; no evidence has been found for any 'tail' of model ages trailing back towards the equiline that are a feature of the Oruanui and Okaia samples.

Oruanui

The Oruanui data are more detailed, in part because of its large volume and also because single pumices yielded sufficient material for analysis. Three datasets are presented, each representing a single pumice clast (Table 1). All three clasts are from the coarser-grained portion of the Oruanui ignimbrite that was erupted during the climactic phase (10) of the eruption (see Wilson, 2001). All three clasts are also of the high-silica rhyolite (74·5–76·0% SiO_2) that is volumetrically dominant (>90%) in the eruption products (Wilson *et al.*, in preparation).

TIMS data

Four sets of TIMS data are presented here: a major-phase set from clast Oruanui 1, and three zircon-controlled sets from clasts Oruanui 1, 2 and 3. The major phases (whole rock, plagioclase, orthopyroxene, hornblende and magnetite) in clast Oruanui 1 yielded a range in ($^{238}U/^{232}Th$) of 0·717–0·802 and ($^{230}Th/^{232}Th$) of 0·738–0·767 (Fig. 7). The corresponding isochron age is 33 +18/–16 ka (MSWD = 2·4). The two-point isochrons in Fig. 8 were constructed from six size-fraction aliquots of zircons: one of <63 μm, three of 63–125 μm, and two of 125–250 μm, plus one bulk aliquot from clast Oruanui 2. In the first six samples, there is a pronounced correlation between the ages and the aliquot grain-size and no significant age differences between aliquots of the same size fractions from two pumices (Fig. 8). Model ages

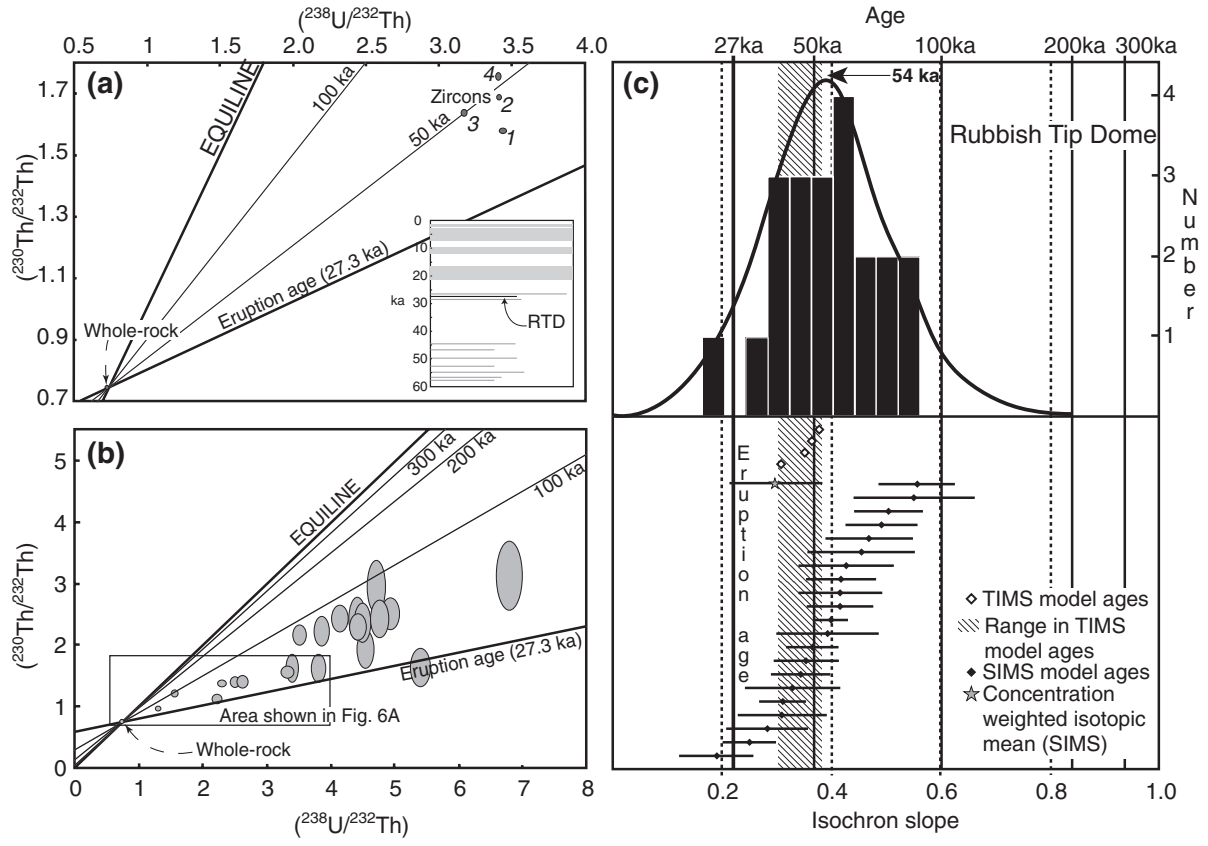

Fig. 6. Data from Rubbish Tip dome samples. (a) TIMS (^{230}Th/^{232}Th) vs (^{238}U/^{232}Th) equiline diagram for bulk zircons and whole rock. Model ages: 1, 40·1 ± 0·6 ka; 2, 47·2 ± 0·7 ka; 3, 49·4 ± 0·9 ka; 4, 51·6 ± 0·8 ka: 2σ errors. (b) SIMS (^{230}Th/^{232}Th) vs (^{238}U/^{232}Th) equiline diagram for single zircons. (c) Rank order plot (bottom) and PDF curve and histogram (top) from SIMS data. Other details as in Fig. 4.

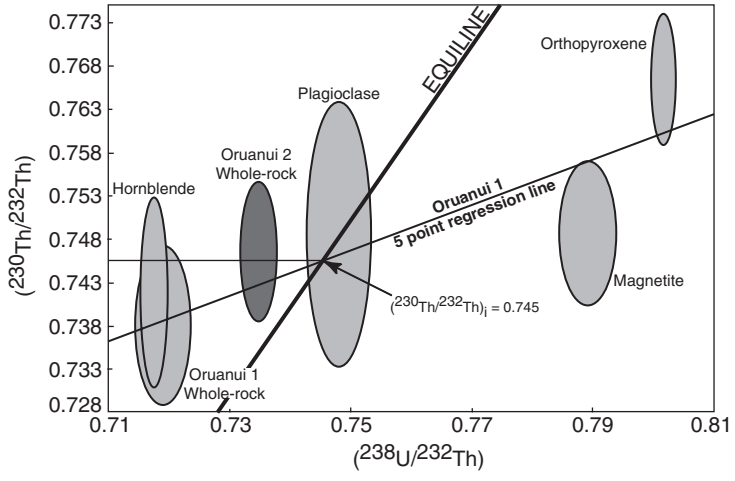

Fig. 7. TIMS (^{230}Th/^{232}Th) vs (^{238}U/^{232}Th) equiline diagram for the major phases and whole rock from sample Oruanui 1, together with the whole-rock value for sample Oruanui 2. A five-point isochron for Oruanui 1 data, fitted using the Monte-Carlo option in Isoplot (Ludwig, 2002), representing an age of 33 +18/–16 ka (MSWD = 2·4) is shown.

range from 32 ± 0·5 ka for <63 μm to 39·6 ± 1 ka for 125–250 μm zircons. The variation in isochron ages with grain size is most pronounced in the Oruanui samples, and has been interpreted to represent either an overgrowth phenomenon or a mixing relationship between two populations of distinctly different ages (Charlier & Zellmer, 2000). Bulk analysis of Oruanui 2 zircons yielded a very similar model age of 38·5 ± 1 ka.

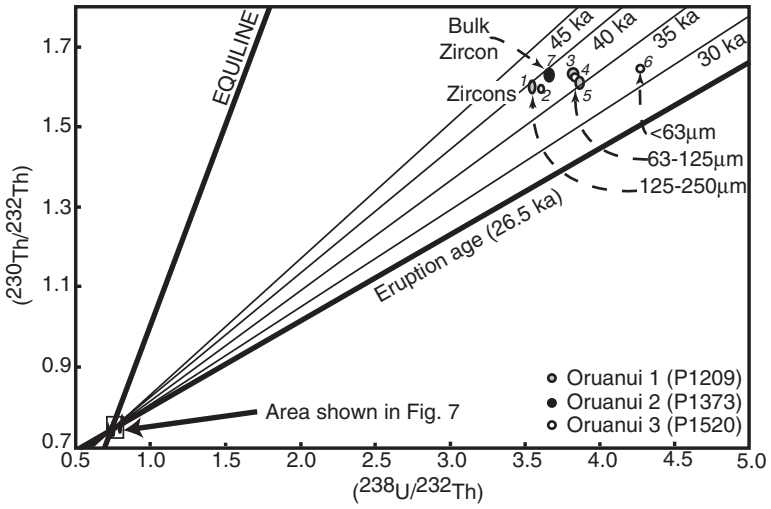

Fig. 8. TIMS (^{230}Th/^{232}Th) vs (^{238}U/^{232}Th) equiline diagram for the zircon size fractions from Oruanui 1 and Oruanui 3, and a bulk zircon separate from Oruanui 2. Model ages: 1, 39·6 ± 1·0 ka; 2, 38·2 ± 0·7 ka; 3, 37·2 ± 0·8 ka; 4, 37·0 ± 0·8 ka; 5, 35·4 ± 0·8 ka; 6, 32·0 ± 0·5 ka; 7, 38·5 ± 1·0 ka: 2σ errors.

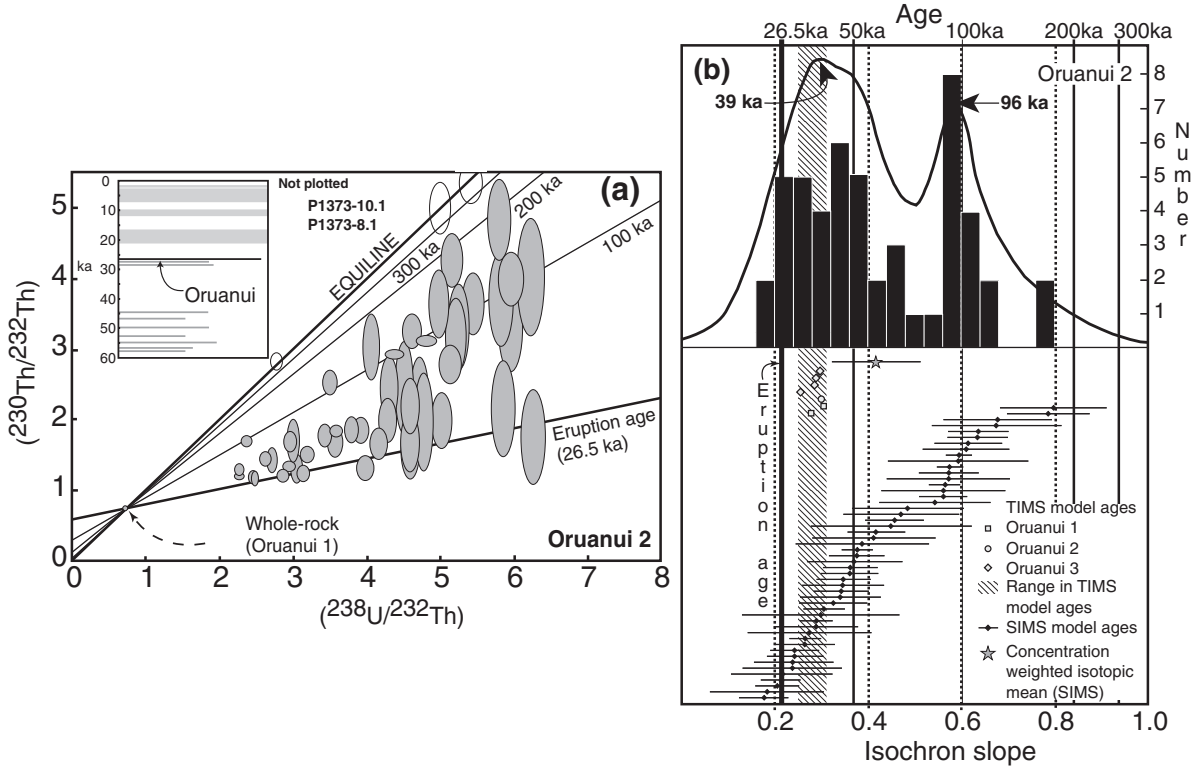

Fig. 9. SIMS data from sample Oruanui 2. (a) (^{230}Th/^{232}Th) vs (^{238}U/^{232}Th) equiline diagram for single zircons. Values used in (b) with grey fill, others (overlapping with the equiline) as open ellipses. (b) Rank order plot (bottom) and PDF curve and histogram (top) from SIMS data. Other details as in Fig. 4.

SIMS data

Fifty and 45 zircons from Oruanui 2 and Oruanui 3, respectively, yielded acceptable age estimates (Figs 9a and 10a). Model-age spectra for each clast (Figs 9b and 10b) show two peaks; a subordinate one at 96 ka and 94 ka, and a dominant younger peak at 39 ka and 32 ka for Oruanui 2 and 3, respectively. The older peaks are indistinguishable from those in the Okaia and Tihoi

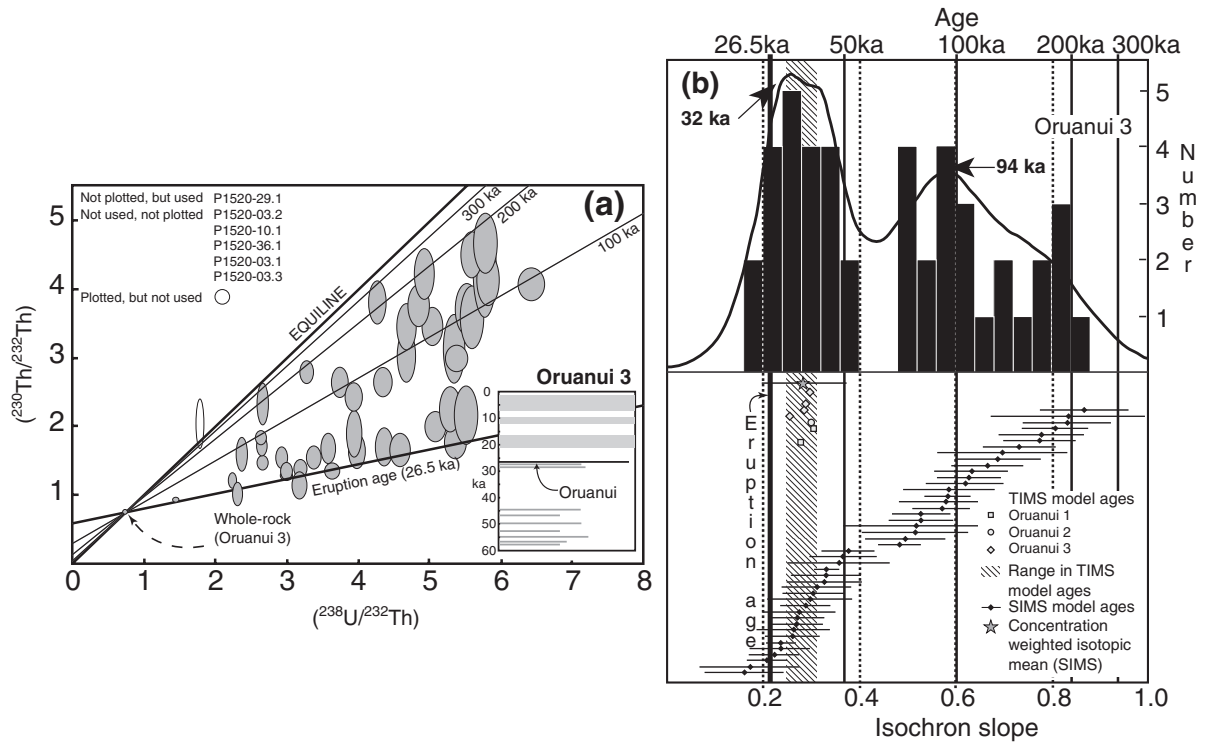

Fig. 10. SIMS data from sample Oruanui 3. (a) (^{230}Th/^{232}Th) vs (^{238}U/^{232}Th) equiline diagram for single zircons. Values used in (b) with grey fill, others (overlapping with the equiline and not used) as open ellipses. (b) Rank order plot (bottom) and PDF curve and histogram (top) from SIMS data. Other details as in Fig. 4.

samples (Figs 4 and 5), and the younger peaks are centred on the 'average' model ages from the TIMS data on samples Oruanui 1 and 3 (Figs 9a and 10a).

Unit Ω

Unit Ω is dacitic and was erupted in the aftermath of the Oruanui eruption, prior to re-establishment of rhyolitic activity (Wilson, 1993; Sutton *et al.*, 2000). Ages of bracketing deposits (Newnham *et al.*, 2003) imply an age of 20 ka. Zircon yields were too low (Table 2) for TIMS analysis, but the grains were analysed by SIMS. Data for many of the grains lie close to or on the equiline in the U–Th system, and were therefore also analysed in the U–Pb system. Six crystals yielded U–Th model ages that were meaningful (Fig. 11), and 12 crystals gave coherent U–Pb model ages that ranged between 244 ka and 524 Ma (Table 3), with two modes. These data are unusual in (1) the diversity of ages, including pre-Quaternary zircons that can only have been derived from basement metasediments, and (2) the presence of cored grains with petrographic (Figs 12a–g) and isotopic evidence for multiple episodes of growth.

Unit B

Unit B, erupted at 11·8 ka, is the earliest post-Oruanui rhyolite at Taupo. Geochemical evidence is consistent with this rhyolite being derived by fractionation from Unit Ω dacite (Sutton *et al.*, 2000) and so data were obtained to compare the age spectra of these two units. The eruption involved several vents spaced along a fissure; material analysed was from fall unit B1, erupted from the earliest and southernmost vent (Wilson, 1993; Fig. 1c).

TIMS data

Five sets of data were obtained from three size fractions: one of <63 μm, three of 63–125 μm and one of 125–250 μm material. All the average ages thus obtained (Fig. 13a) are younger than the 26·5 ka Oruanui eruption age: the largest grain-size fraction yielded 23·8 ± 0·6 ka, whereas ages from the intermediate and smallest grain-size fractions ranged from 18·7 ± 0·5 to 16·0 ± 0·9 ka. There is thus evidence for a grain-size dependence of model ages, but this is much less clear-cut than in the Oruanui data (Fig. 8).

SIMS data

Twenty-seven data points gave meaningful ages (Fig. 13b and c). The age spectrum is dominated by <50 ka zircons, but with weakly bimodal probability peaks at 23 ka and 34 ka that are within error of, and older than, the TIMS average ages, respectively (Fig. 13a). Only five

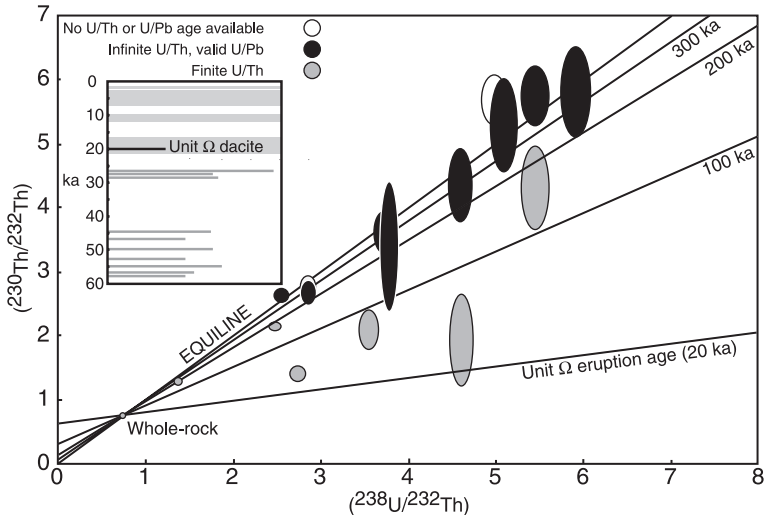

Fig. 11. SIMS ($^{230}Th/^{232}Th$) vs ($^{238}U/^{232}Th$) equiline diagram for zircons from Unit Ω. Open symbols denote analyses for which no U–Th or U–Pb age information is available, black symbols indicate analyses where no U–Th age information but meaningful U–Pb ages are available. Grey symbols indicate analyses where meaningful U–Th ages could be determined. Other details as in Fig. 4.

Table 3: Compilation of U–Pb data for samples P1158 (Unit G) and P1106 (Unit Ω) (see Electronic Appendix 3 for more details)

Spot name	Site	Fig. 12	Age (Ma)	1σ error
Unit G				
P1158-9	—	—	91·7	4·1
P1158-5	—	—	134·9	2·5
P1158-12	—	H	206·9	3·8
P1158-14·1	—	—	419·8	7·3
P1158-15	—	I	527·4	9·1
Unit Ω				
P1106-11	—	C	0·244	0·051
P1106-14	—	—	0·265	0·065
P1106-5-1	Core	E	523·6	10·0
P1106-5	Rim	E	0·323	0·155
P1106-15-4	Core	A	111·1	2·2
P1106-15-4r	Rim	A	0·343	0·098
P1106-10	—	—	0·369	0·077
P1106-15	Core	—	0·375	0·025
P1106-15-5	Rim	D	0·454	0·034
P1106-9	—	G	0·464	0·071
P1106-13-1	Core	C	371·1	6·9
P1106-13	Rim	C	0·473	0·031
P1106-6	—	F	0·513	0·112
P1106-2	—	B	108·3	2·1
P1106-3	—	—	254·8	5·6
P1106-15-1	Core	—	357·4	6·3

crystals yielded model ages of >50 ka. Two of these are in the same 90–100 ka age bracket as the older zircon population that is more clearly defined in the Tihoi, Okaia and Oruanui samples. The oldest grain (195 ka; P1157-19) yielded U and Th concentrations of 6500 and 10 000 ppm, respectively (Electronic Appendix 2) and was excluded from the concentration weighted mean (Fig. 13c) because addition of this sample alone skewed the mean from 31 +12/–11 to 46 +14/–12 ka and out of error with the TIMS bulk average ages.

Unit D (Acacia Bay dome)

Unit D is a fall deposit generated during minor explosive activity accompanying growth of a dome at Acacia Bay at 11·4 ka (Wilson, 1993; Fig. 1c). This dome is unusual in the post-Oruanui sequence for being situated outside the main concentration of other vents (Wilson, 1993), and is more crystal-rich (5–8%) and geochemically variable than other eruptive units from ~12 to 1·8 ka (Sutton *et al.*, 2000). The pumiceous dome carapace was sampled for this study. Only sufficient zircons for two aliquots of 63–250 μm grain size could be obtained for TIMS work, and no SIMS data were obtained. Model ages (Fig. 14) are slightly older than those from Units B and E, and similar to the eruption age of the Oruanui and thus the younger peak in model ages of the Oruanui rhyolites (Figs 9a and 10a).

Unit E

Unit E is the last (erupted at 10·0 ka) and largest deposit of the first post-Oruanui rhyolite magma

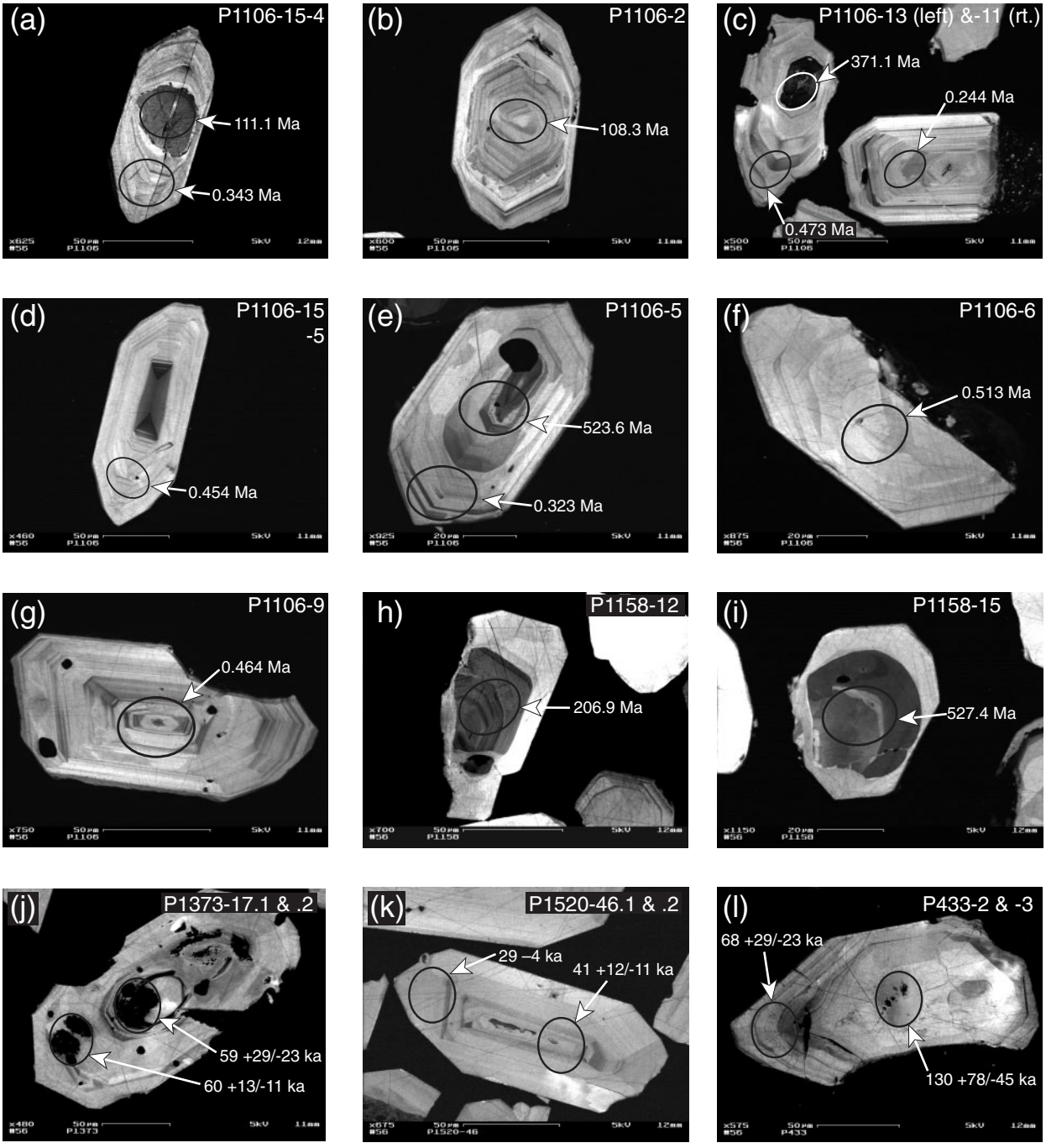

Fig. 12. Cathodoluminescence images of zircons from Unit **Ω** (a–g), and Unit G (h and i). (j–l), examples of zircons from other units where analysis of core vs rim showed that there were no significant age differences in the U–Th system (j and k, Oruanui) and a significant difference (l, Tihoi). Plates are annotated with grain number and the approximate location of the SIMS analysis, with the corresponding age determination for that location.

batch (Wilson, 1993; Sutton *et al.*, 2000). Material analysed was from fall unit E1, erupted from the westerly of the two vents active in succession in this eruption (Wilson, 1993). Thus the first post-Oruanui rhyolite batch is represented here by material erupted from vents as widely spaced as possible, to test for any geographical variations in characteristics (compare Rubbish Tip dome with Okaia and Oruanui: Fig. 1b). The zircon yield (Table 2) was sufficient for only TIMS analysis.

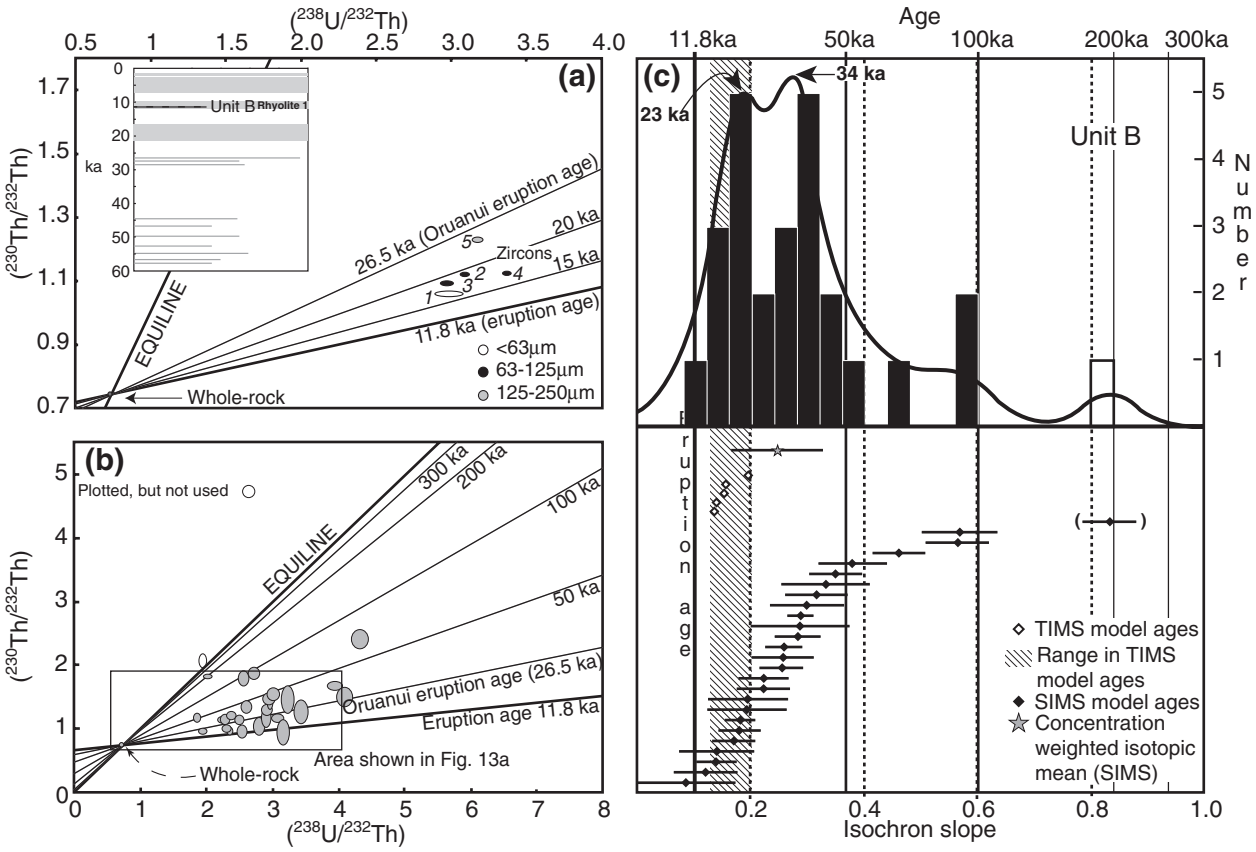

Fig. 13. Data from Unit B samples. (a) TIMS (^{230}Th/^{232}Th) vs (^{238}U/^{232}Th) equiline diagram for bulk zircons and whole rock. Model ages: 1, 16·0 ± 0·9 ka; 2, 18·7 ± 0·5 ka; 3, 18·2 ± 0·7 ka; 4, 16·6 ± 0·4 ka; 5, 23·8 ± 0·6 ka: 2σ errors. (b) SIMS (^{230}Th/^{232}Th) vs (^{238}U/^{232}Th) equiline diagram for single crystals. Values used in (c) plotted with grey fill; others overlapping with the equiline as open ellipses. (c) Rank order plot (bottom) and PDF curve and histogram (top) from SIMS data. Other details as in Fig. 4.

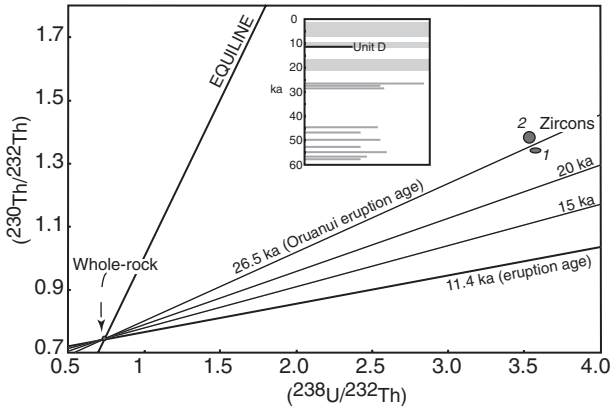

Fig. 14. TIMS (^{230}Th/^{232}Th) vs (^{238}U/^{232}Th) equiline diagram for Acacia Bay dome (Unit D) zircons and whole rock. Model ages: 1, 25·4 ± 0·6 ka; 2, 27·9 ± 1·1 ka: 2σ errors. Other details as in Fig. 4.

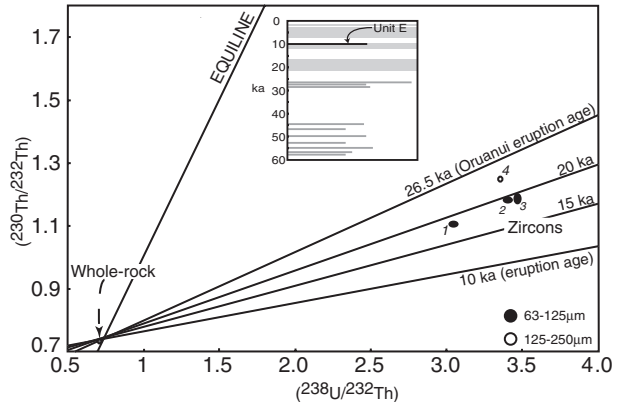

Fig. 15. TIMS (^{230}Th/^{232}Th) vs (^{238}U/^{232}Th) equiline diagram for two size fractions of Unit E zircons and whole rock. Model ages: 1, 18·9 ± 0·6 ka; 2, 19·9 ± 0·5 ka; 3, 19·6 ± 0·7 ka; 4, 23·6 ± 0·5 ka: 2σ errors. Other details as in Fig. 4.

TIMS data

Four zircon aliquots were obtained in two size fractions: three samples of 63–125 μm and one of 125–250 μm. As with Unit B (Fig. 13a), the average ages obtained (Fig. 15) are younger than the 26·5 ka Oruanui eruption age. The larger grain-size fraction yielded 23·6 ± 0·5 ka, whereas the smaller fractions ranged from 19·9 ± 0·5 to 18·9 ± 0·6 ka. Both groups of model ages are very close to or

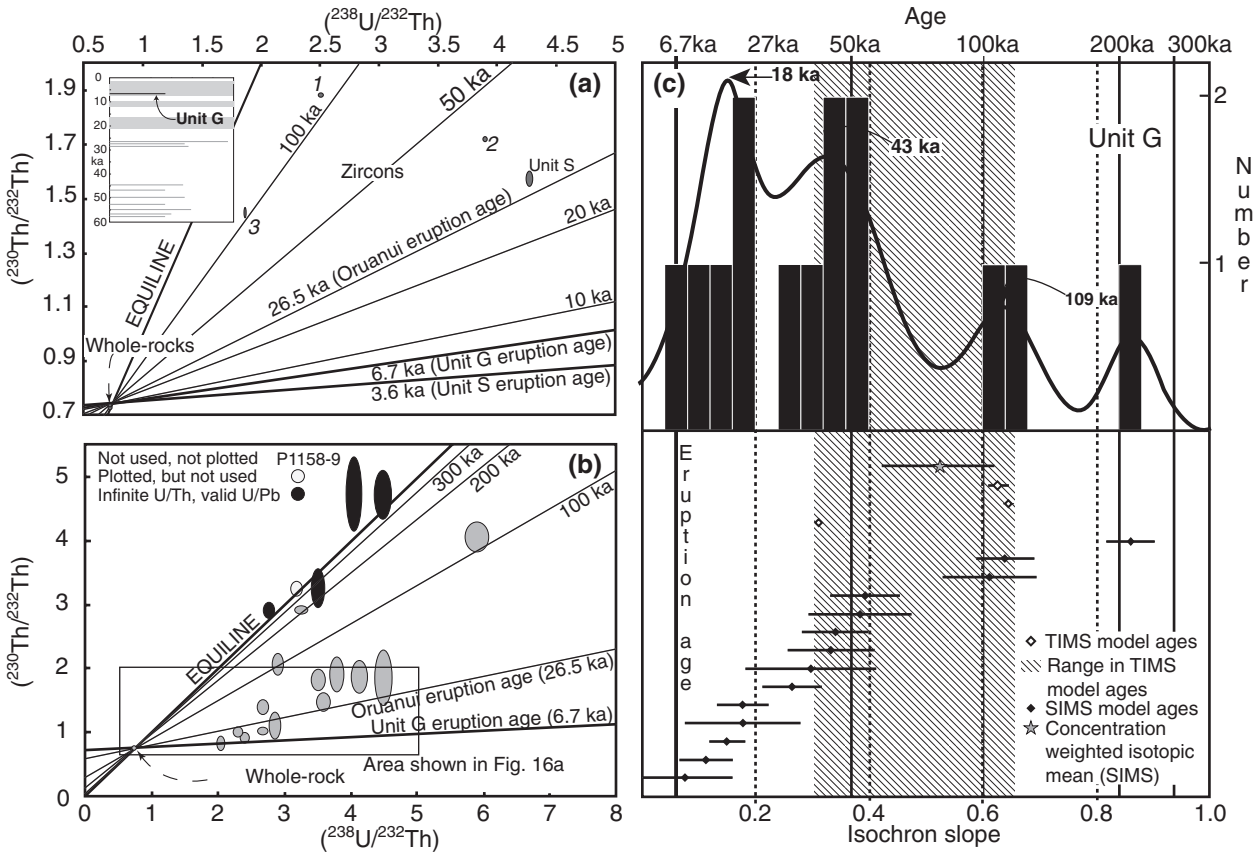

Fig. 16. (a) TIMS ($^{230}Th/^{232}Th$) vs ($^{238}U/^{232}Th$) equiline diagram for Unit G zircons and whole rock. Model ages: 1, 113·2 ± 3 ka; 2, 40·7 ± 0·7; 3, 107·8 ± 5·4 ka: 2σ errors. Corresponding data point for Unit S is plotted; this has a model age of 29·7 ± 1·1 ka, 2σ error. Unit S (3·6 ka), Unit G (6·7 ka) and Oruanui (26·5 ka) eruption age isochrons plotted for reference. (b) SIMS ($^{230}Th/^{232}Th$) vs ($^{238}U/^{232}Th$) equiline diagram for Unit G analyses. Values used in (c) plotted with grey fill, others overlapping with the equiline as open ellipses. Black ellipses denote U–Th infinite age analyses that gave meaningful U–Pb ages (Table 3 and Electronic Appendix 3). (c) Rank order plot (bottom) and PDF curve and histogram (top) for Unit G SIMS data. Other details as in Fig. 4.

overlapping with those from the analogous grain-size fractions in Unit B (Fig. 13a), with again some evidence for a grain-size dependence of model ages.

Unit G

Unit G, erupted at 6·7 ka, is the oldest-but-one deposit from the second post-Oruanui rhyolite batch (Wilson, 1993; Sutton *et al.*, 2000). The inferred vent site is nearly coincident with that for material sampled here from Unit B (Wilson, 1993; Fig. 1c), but Units B and G have distinctly different chemical compositions (Sutton *et al.*, 2000). The Unit G zircon yield (Table 2) was much lower than for samples from the first post-Oruanui rhyolite batch.

TIMS data

Three zircon aliquots were analysed, each containing material from 63 to 250 μm in grain size. The model ages (Fig. 16a) differ markedly from those of the other post-Oruanui rhyolites; all pre-date the Oruanui eruption, and have a wide, non-systematic scatter of values, from 40·7 ± 0·7 ka to 113·2 +3·0/–2·9 ka.

SIMS data

Fourteen crystals gave meaningful ages (Fig. 16b); other older crystals within error of the equiline were also analysed by U–Pb methods. U–Th model ages range from 9 ka to >∼350 ka (Electronic Appendix 2); U–Pb ages range from 92 to 527 Ma (Table 3). The U–Th SIMS age distribution has dominant young peaks at 18 ka and 43 ka, and a smaller older peak at 109 ka (Fig. 16c). The mean values yielded by TIMS show the apparent dominance of the younger peaks to be spurious.

Unit S (Waimihia)

Unit S, also known as the Waimihia Tephra and erupted at 3·6 ka, is the most voluminous eruption of the second post-Oruanui rhyolite magma batch (Blake *et al.*, 1992; Sutton *et al.*, 2000). Sufficient zircons could be extracted for only one TIMS analysis (Table 2), which yielded a

model age of 29·7 ± 1·1 ka (Fig. 16a), substantially different from the ages obtained for Unit G, and similar to the younger peak in model ages obtained from the Oruanui.

Unit Y (Taupo)

Unit Y was generated during the 1·8 ka Taupo eruption, and in total is larger than all the other post-Oruanui eruptives combined (Wilson & Walker, 1985; Wilson, 1993). No zircons were obtained from an ~15 kg sample of pumices from the second (Taupo plinian) pumice fall deposit in this eruption, and a three-point isochron from whole rock and two magnetite fractions gave an age of negative 12·6 +20·2/–16·7 ka (Charlier, 2000).

DISCUSSION

The zircon age data presented above comprise three contrasting datasets.

(1) Multi-crystal TIMS ages that are precise, but that must be treated with caution as they represent averages, weighted by the U and Th concentrations in the individual crystals, and may vary with grain-size fraction, indicating overgrowth or mixed populations.

(2) Single-crystal SIMS U–Th ages that are less precise, but yield data on the spectrum of ages and U and Th concentrations present in a given zircon population. Although individual crystals commonly show complex growth patterns under CL (Fig. 12), there is no significant variation in core vs rim model U–Th ages in crystals with euhedral cores large enough to permit separate analyses (e.g. Fig. 12j and k). In most cases zircon crystals were not large enough to permit core vs rim analyses, and the beam spot was centred on the crystal core. Only in crystals with partly resorbed cores, distinguishable by CL, did samples yield significantly older core ages (resolvable by U–Pb dating: Table 3).

(3) Single-crystal SIMS U–Pb ages (Table 3) in two samples (Units Ω and G) that indicate the presence of two older zircon populations: one of Quaternary age, dating back to 0·513 ± 0·112 Ma (see Brown & Fletcher, 1999), the other of Mesozoic and Palaeozoic age, ranging between 91·7 ± 4·1 and 527·4 ± 9·1 Ma.

These datasets are discussed below in three contexts: (1) controls on the zircon populations in the Taupo magmas; (2) implications of the age spectra for the evolution of the Taupo system and the nature of the local crust; (3) consequent implications for the dynamics of large caldera-forming silicic magmatic systems.

Zircon abundances and chemistries, and their influence on model-age spectra at Taupo

Although only a small minority of zircons in the Taupo deposits show evidence for multiple episodes of growth and/or dissolution, the zircon populations from all but one sample represent at least one episode of growth superimposed on earlier possible episodes of growth and/or dissolution. Interpretation of the zircon age spectra at Taupo requires consideration of the controls on zircon growth or dissolution, the influence of these controls on zircon abundances in each deposit, and the absolute abundances of U and Th in the zircons.

Controls on zircon growth and dissolution

The model-age populations reported here are made up of zircons that crystallized at, or shortly prior to, the moment of eruption and older grains, some resolvable into particular age suites (e.g. the older peak in the Tihoi, Okaia and Oruanui) and others ranging in age back to the Palaeozoic. The only exception is the Rubbish Tip dome, where a single population is present (Fig. 6). In sample processing, zircon yields varied by about three orders of magnitude (Table 2), and the nature of the associated age population varies quasi-systematically with the yield. We explain these relationships by considering the state of zircon saturation in the magmas.

For each of the samples, two temperatures can be defined. The magma temperature can be derived from Fe–Ti oxide equilibria (T_{oxide}: Ghiorso & Sack, 1991) and an estimate can also be made of the temperature at which zirconium saturation occurs in the melt and zircon crystallization commences (T_{zirc}: Watson & Harrison, 1983). The latter depends on the Zr content of the melt and the cation ratio [M, defined as (Na + K + 2Ca)/(Al × Si)] (Watson & Harrison, 1983). Although glass analyses are used where available (Sutton, 1995), use of whole-rock compositions does not significantly change estimates of T_{zirc} [e.g. clast Oruanui 1: T_{zirc} (glass) = 773°C (where M = 1·28 and Zr = 136 ppm), vs T_{zirc} (whole rock) = 775°C (where M = 1·26 and Zr = 147 ppm)]. In Fig. 17, estimates of T_{zirc} and T_{oxide} are used to divide the samples into three categories.

(1) $T_{oxide} < T_{zirc}$. Here, zircon was crystallizing at the time of eruption. Samples from the Oruanui and the first post-Oruanui rhyolite batch (Units B and E, and the Acacia Bay dome) fall into this category. All four samples share young average (TIMS) zircon ages, which are within 10–15 kyr of the eruption age (Figs 9a, 10a, 13a and 14), and three of them contain a dominantly young population of crystals (Figs 9c, 10c and 13c).

(2) $T_{oxide} \approx T_{zirc}$. Here, zircon may have been crystallizing when eruption occurred, but the younger population thus formed is not so abundant that it swamps any older, possibly inherited, population. Any older crystals neither grew nor dissolved appreciably in the magma and could, in principle, have survived indefinitely. Samples from the Tihoi, Okaia and Rubbish Tip dome, and the second post-Oruanui

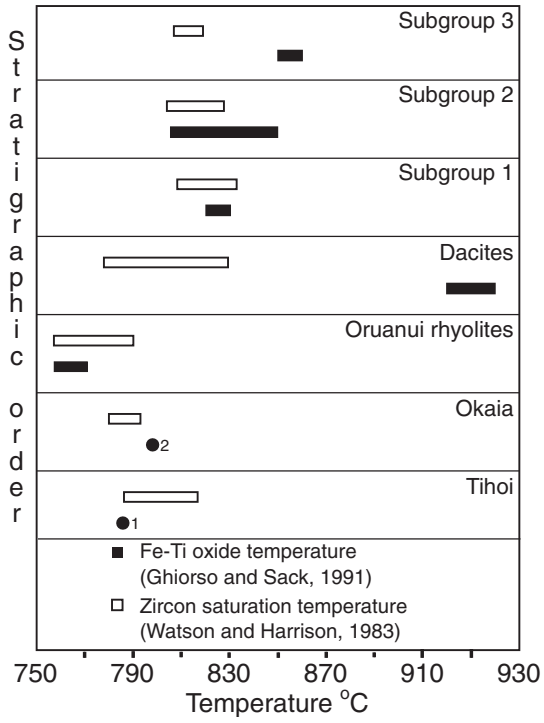

Fig. 17. Plot of temperature estimates by Fe–Ti oxides (Ghiorso & Sack, 1991) and estimated zircon saturation temperatures (Watson & Harrison, 1983) vs stratigraphic ordering for the units sampled in this work. Where possible, glass analyses are used for zircon saturation temperature calculations (see text). Numbered Fe–Ti oxide temperature data points: (1) from Shane (1998); (2) from Dunbar *et al.* (1989*b*). All other data from Sutton (1995) and Sutton *et al.* (2000).

rhyolite group (Units G and S) are in this category. They all have TIMS model ages that are tens of kyr older than the eruption age (Figs 4, 5, 6 and 16), and (in cases where there are two age modes) have comparable proportions of younger and older zircons (Figs 4c, 5c, 6c and 16c).

(3) $T_{oxide} > T_{zirc}$. Here zircon was at the time of eruption likely to be dissolving and only old crystals were present, if they had not already dissolved. Unit **Ω** is in this category and its zircon population is dominated by crystals that are much older than eruption age.

Pre-350 ka Quaternary and older inherited zircons, revealed in SIMS data, have been found only in Units **Ω** and G, i.e. in samples where little (G) or no (**Ω**) young zircon crystallization has occurred. We suspect that older zircons could be present in the other eruptives, but their presence is masked by the abundance of younger crystals. The zircon abundance in Unit **Ω** is $\sim 10^3$ times less than in the Oruanui, so that in our suite of ~100 Oruanui zircons the probability of finding a >350 ka zircon is very low. Thus the role of new vs inherited zircons in rhyolites in the TVZ (e.g. Lindsay *et al.*, 1994; Brown & Fletcher, 1999), and hence rhyolite petrogenetic processes, cannot be considered without first considering the host rock chemistry and the origins of its zircon crystal population.

The preservation of older zircon populations requires zircon dissolution to have been minimized in the Taupo eruptives. Two factors are important here. First, the incorporation into magma of zircons from an earlier partly to wholly crystallized plutonic, or metasediment, host requires disaggregation of the host rock, probably through significant degrees (tens of volume per cent) of melting. Second, the composition of the resulting melt (whether pure assimilant or mingled with the melting agent; see below) will then dictate whether the liberated zircons will dissolve or grow.

The optimal conditions for large-scale melting of country rock are attained when hot mafic magma is intruded in large volume into the crust (Huppert & Sparks, 1988*a*, 1988*b*; Koyaguchi & Kaneko, 1999). If mantle-derived mafic melts are mingled with crust-derived felsic melts, the resulting composition is likely to be basaltic andesite to andesite (McCulloch *et al.*, 1994) and zircon undersaturated. Such compositions do occur at Taupo in the time period considered here. Two andesitic lineages occur in the Oruanui (Sutton *et al.*, 1995; Wilson *et al.*, in preparation) and andesite occurs in Unit S (Blake *et al.*, 1992); all three andesites are strongly zircon undersaturated. Any evolutionary pathway involving such magmas as the parental compositions (McCulloch *et al.*, 1994) is thus most unlikely to preserve any assimilated zircons through to rhyolitic compositions (Watson, 1996). However, if the melted country rock does not mingle with any mafic magma (Huppert & Sparks, 1988*a*, 1988*b*), then zircon dissolution may be negligible, or growth may occur, both because of bulk compositions of the crustal melt [which at Taupo are likely to be zircon saturated or nearly so; see Palmer *et al.* (1995)] and the rapidity with which the melt cools to a temperature similar to the melting range of its crustal source (Koyaguchi & Kaneko, 1999).

We model these possibilities by using the zircon dissolution–growth model of Watson (1996), applied to four Taupo compositions: the most mafic Oruanui basaltic andesite, Unit **Ω** dacite, Unit G rhyolite, and Unit Y rhyolite. The first and last of these lack zircons, whereas the other two zircon populations are dominated by inherited grains. Values for melt viscosity were calculated (Shaw, 1972) assuming a conservative H_2O content of 3 wt % and these were then used to calculate Zr diffusivity (Mungall, 2002). Numerical simulations (Watson, 1996) using these Zr diffusivity values were used to estimate zircon dissolution rates in the various melt compositions for spherical 'crystals' of initial radii 250, 125 and 63 μm (Table 4).

Zircons in the Oruanui mafic composition are predicted to dissolve rapidly. This result strongly counts against any genetic model invoking fractionation from such contaminated mafic parents (McCulloch *et al.*, 1994) for the origin of rhyolites such as Unit G (where old zircons survive). Given the geochemical similarities,

Table 4: Parameters and results for zircon dissolution modelling using the methods of Watson (1996), applied to (1) the least-evolved Oruanui mafic compositions, (2) Unit Ω dacite, (3) Unit G rhyolite, and (4) Taupo (Unit Y) rhyolite (see text for details)

Sample	Rock type	M value	Zr (ppm)	U_0	Fe–Ti oxide temp. (°C)	Initial radius (μm)	Time to disappearance (yr)
P561	Oruanui basaltic andesite	2·07	165	994	925	63	0·2
						125	0·9
						250	3·7
P1106	Unit Ω dacite	1·50	236	514	930	63	6
						125	24
						250	96
P1158	Unit G rhyolite	1·39	231	26	830	63	1520
						125	6040
						250	24000
Y5 glass	Unit Y rhyolite	1·40	225	113	855	63	760
						125	3000
						250	12000

such models can be excluded for most of the rhyolites considered here. The largest zircons will also dissolve in <100 yr in the Unit Ω dacite. Such a time period is much shorter than the gaps between the three post-Oruanui dacite eruptions (Wilson, 1993). This and the subhedral to euhedral morphologies of the zircons (which are up to 250 μm in size) imply that the Unit Ω dacite must have been erupted ≪100 years after the introduction of the zircons to the dacite magma. In Unit G, the largest zircons will dissolve in 24 kyr, a period much longer than the gaps between individual eruptions or magma batches around that time, and any inherited material should be expected to be preserved. For Unit G this is the case, Mesozoic- to Palaeozoic-aged zircons are found, and these have not been swamped by a new younger population as the degree of zircon saturation is neutral to negative. For Unit Y, the largest zircon fraction would dissolve in ~12 kyr and, for the same reasons as for Unit G, it should be expected that inherited zircons would be preserved. However, no zircons were found in Unit Y, implying that this rhyolite batch had an evolutionary history that had stripped out any inherited zircons (e.g. at higher temperatures, see Fig. 17, or through melting of zircon-poor sources) and that it remained sufficiently Zr-undersaturated to preclude crystallization of new zircons.

Relationship between zircon sizes, compositions and ages

The SIMS and TIMS data show that, in addition to the wide range of model ages, the absolute concentrations of U and Th vary by about an order of magnitude [as also reported by Brown & Fletcher (1999)]. In the SIMS data, there will be a lower cut-off of U concentrations, below which the technique cannot resolve the age of a grain, but this will apply (to a first order) evenly over the age range covered by the U–Th disequilibrium system and we infer this does not impart a systematic bias. A previously undocumented effect is that the TIMS average model ages will be significantly influenced by the variable distribution of U and Th abundances between older and younger populations, or between smaller and larger crystals.

In the Okaia and Oruanui samples, two zircon age populations are prominent, one with a mode around 100 ka, and a younger one that is close to the eruption age (Figs 5c, 9b and 10b). However, the TIMS model ages differ substantially, being virtually coincident with the PDF peak for the younger population in the Oruanui, but significantly older in the Okaia (Fig. 18). This could reflect the dominance of crystals from the younger age population, as well as the fact that the younger population is concentrated in smaller grain sizes in the Oruanui vs the Okaia (see Figs 5 and 8; Charlier & Zellmer, 2000).

In addition, the role of variable U and Th abundances will skew results if the variations are systematic with respect to crystal age or size. Such appears to be the case in all the <250 ka zircons analysed in this study (Fig. 19), where peaks in U and Th abundance occur that are coincident with the peaks in age determinations. The fact that U and Th behave similarly precludes periodic influxes of U-rich slab-derived fluids as a cause for such variations (see Hawkesworth *et al.*, 1997). One possible explanation is that zircons that crystallized at certain

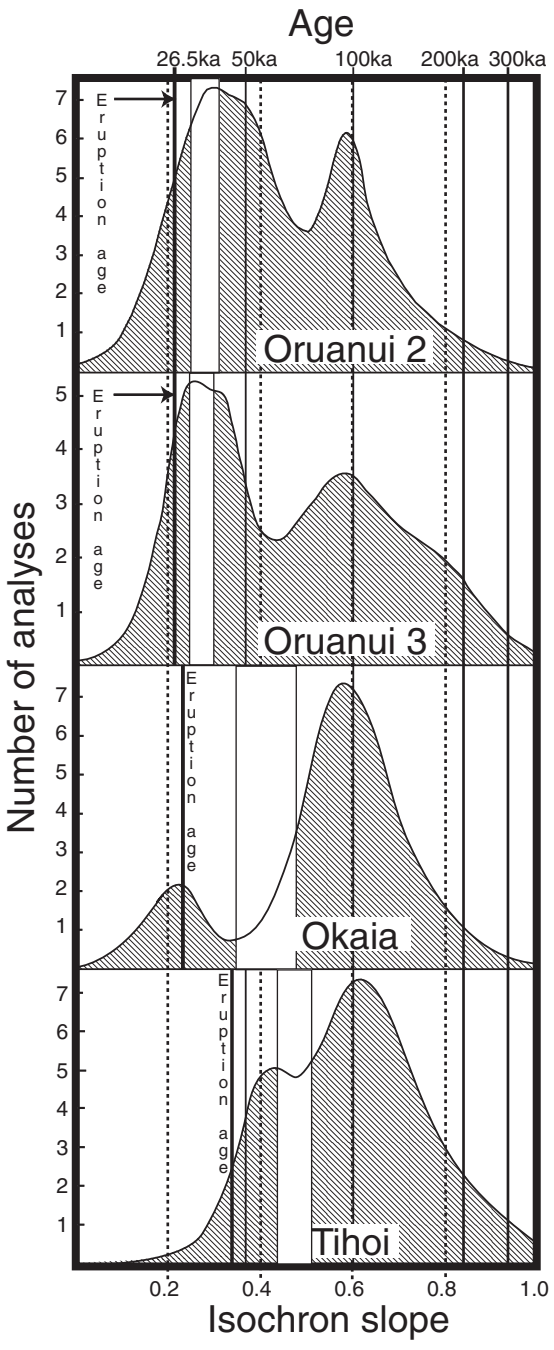

Fig. 18. Compilation of PDF curves from Tihoi, Okaia, Oruanui 2 and Oruanui 3 SIMS data (Figs 4, 5, 9 and 10), stacked vertically for comparisons of the peaks in maximum probability through the sequence. Ranges in TIMS model-age data for each sample are represented by the white band.

times were formed in larger bodies of crystal-poorer, zircon-saturated melt that encouraged zircon nucleation and growth, and allowed the zircons to sequester more U and Th from the melt.

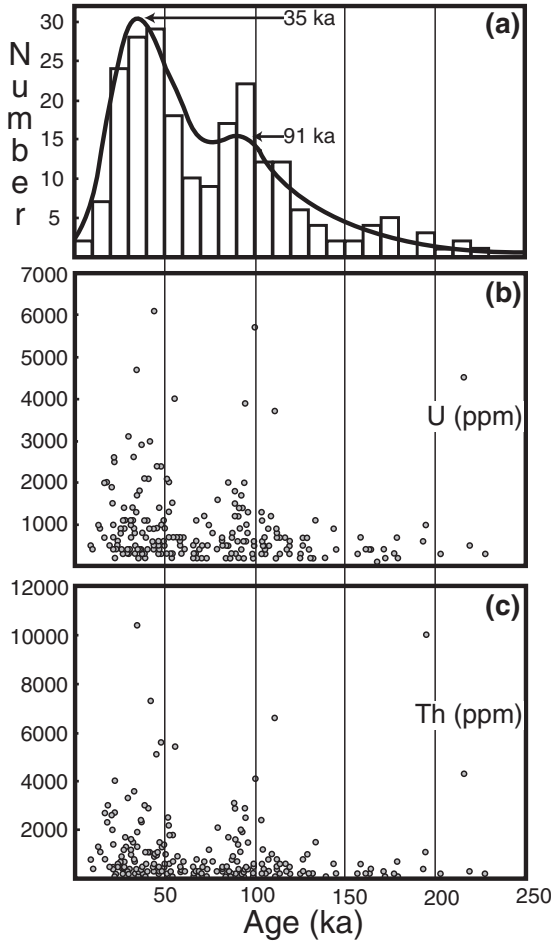

Fig. 19. (a) Cumulative probability density curve and histogram based on isochron slopes derived from two-point whole-rock–zircon determinations from all SIMS U–Th data, except for unit Ω, that yield finite ages ($n = 220$). Maxima in the probability curve at 35 ka and 91 ka are annotated. (b) and (c) Plots of U and Th concentrations, respectively, vs model age (from SIMS U–Th data, i.e. up to 250 ka) for individual zircons from all Taupo eruptives to show common peaks in U and Th concentrations at ~100 ka and 35 ka.

Temporal evolution of Taupo volcano

Contrasting magmatic systems and crustal sources at >26·5 ka

During the ~40 kyr over which the Oruanui-type rhyolite was erupted, at least two other distinct rhyolites were erupted from adjacent sources (Sutton *et al.*, 1995; Wilson *et al.*, 2002: Fig. 3). In particular, the 'NE dome' magma type of Sutton *et al.* (1995), which gave rise to two fall deposits at >45 ka (unnamed) and 27·3 ka (Poihipi), together with domes at Ngangiho and Trig 9471 plus Rubbish Tip, respectively, is distinct from the Oruanui type. However, the vent sites are only ~14 km apart (Fig. 1b). The zircon model-age spectra support the notion that these two magma types represent wholly distinct magmatic systems, even though contemporaneously

active and closely spaced. The Rubbish Tip dome has zircons with a unimodal model-age spectrum, with no recycled TVZ or greywacke components, consistent with magma production in a single generation and crystallization event. Similarities between the 'NE dome' compositions suggest a common source, but the distance between the individual domes is similar to the distance from any one of them to the Oruanui vent sites (Fig. 1b). It thus seems unlikely that these NE domes represent tappings off a single large magma body. Instead, the Rubbish Tip dome (plus Poihipi Tephra and Trig 9741 dome) is interpreted to represent an isolated body of magma that was generated within a source region that chemically and isotopically was the same as that for the Ngangiho dome (hence >15 km across), but separate in other respects from the Oruanui system.

Build-up to the 26·5 ka Oruanui eruption

Magma similar to the dominant volume of rhyolite erupted in the Oruanui event was first erupted around 65 ka (Sutton *et al.*, 1995). The two largest pre-climactic eruptions of this Oruanui-type magma were the Tihoi and Okaia, each representing ~3 km^3 dense rock equivalent (DRE). It is logical to consider these eruptions as early leaks from a growing magma body that erupted climactically at 26·5 ka. However, the zircon data suggest that such a view is questionable.

The corresponding SIMS datasets (Figs 4c, 5c, 9b and 10b) show two peaks in the PDF curves (Fig. 18). In all three units, a common peak at 94–104 ka is accompanied by a younger peak that corresponds more closely to the respective eruption age. The relationship in the Oruanui between the zircon grain sizes and model ages (Fig. 8) can be treated as due to either overgrowth of a pre-existing crystal population by a rapid period of crystallization (that also nucleates and grows a new suite of smaller zircons), or a mixing relationship between two crystal populations where the older one has a coarser grain-size distribution (Charlier & Zellmer, 2000). The bimodality in the SIMS ages (Figs 9 and 10) and U-concentration data (Fig. 19) suggests that the latter is the case, but this has a very important implication. The model ages represented in the younger Tihoi PDF peak are effectively absent from the Okaia and Oruanui model-age spectra. If all three magmas were evolving in the same chamber, then the episode of zircon growth just prior to the Tihoi eruption at ~45 ka should be represented by a peak in crystals of that age in the later two eruptions. However, such zircons are effectively absent. In addition, similar zircon yields for the Tihoi, Okaia and Oruanui samples (Table 2) preclude the younger peak in the Oruanui simply being due to an additional episode of growth superimposed on the magma represented by the Tihoi and Okaia. This implies that the shortly pre-eruptive crystallization episodes undergone by the magmas in these eruptions (or, at least, the Tihoi vs the Okaia plus Oruanui) were in each case confined to the magma volume involved in that particular eruption. Thus, although linked to the magmas involved in later eruptions, the Tihoi magma underwent its late-stage evolution in isolation, not as part of a larger growing magma chamber. Any distinction between the Okaia and Oruanui bodies is not resolvable with the Zr model-age data.

Post-26·5 ka sequence: evolution and relationship to Oruanui

The post-26·5 ka sequence represents a compositional break with the Oruanui, even though most of the younger vent sites overlie the Oruanui caldera outline (Sutton *et al.*, 1995, 2000; Fig. 1c). The model-age spectra of the post-Oruanui deposits are mostly explicable by considering the effect of zircon saturation on whether or not any older population is overprinted by a younger period of zircon growth (Fig. 17). In Unit B, which has the greatest proportion of younger zircons (Fig. 13c), the young population shows a double peak in PDF values over an age range that is very similar to that of the single younger peaks in the Oruanui and Okaia eruptives (Fig. 18). On this basis alone it could be argued that the first post-Oruanui rhyolite batch (and its parental dacite) was being generated from the same source region as the Oruanui and its precursors at the time when the Oruanui rhyolite was accumulating at a higher level prior to eruption. However, the chemical and isotopic characteristics of the post-26·5 ka eruptives are uniform within their respective batches, and show no mixing trends towards Oruanui compositions (Sutton *et al.*, 2000). In addition, the TIMS zircon ages for Unit B are all younger than 26·5 ka (Fig. 13a), and the U/Th ratios of Unit B zircons are, on average, lower than for the Oruanui (see Figs 9a, 10a and 13b). We conclude that although the source region(s) for the post-26·5 ka magmas contained zircons that crystallized at the same time as those in the Oruanui (as well as two zircons of ~100 ka age), the two sets of zircons and the corresponding source zones were distinct in some way.

Contrasts in zircon model-age spectra between samples from Unit Ω and the first rhyolite batch (Units B and E and the Acacia Bay dome) are interpreted to reflect the dominance of young zircon growth in the latter, shown in the 200–500 times greater zircon yields (Table 2). Our SIMS sample sets were not large enough for the rhyolites to determine if they also contained any old zircons, but geochemical evidence suggests that the dacites and rhyolites are genetically linked. The wide geographical spacing of vents for the batch 1 samples (Fig. 1c) is not reflected in any model-age differences. Contrasts in model-age spectra between rhyolites of batches 1 and 2

(Units G and S) can also be related to the zircon saturation state of the magmas (Fig. 17) and consequent zircon abundances (Table 2), such that the batch 2 rhyolites have older average ages. In particular, Unit G also contains basement-derived zircons, implying that its generation involved crustal lithologies of comparable ages to those for Unit **Ω**, over similar geographical areas (Fig. 1c), despite the differences in composition of the rhyolites of batches 1 and 2.

Nature of the source region and implications for rhyolite genesis at Taupo

Nature and age of the deep crust at Taupo

Available evidence suggests that rocks with seismic characteristics appropriate to quartzo-feldspathic densities and compositions ($V_p \approx 6{\cdot}1$ km/s) pass downwards into denser lithologies ($V_p \approx 7{\cdot}1$ km/s) at ~15 km depth below Taupo (Stern & Davey, 1987; M. Reyners, personal communication, 2003). Thus any zone for felsic crustal melting contributing to the silicic magmas realistically has to lie at or above that level. Foundering of residual and/or refractory material to >15 km depths is very likely, but such material is then unlikely to be involved in further large-scale melting. Direct generation of significant volumes of silicic melts from >15 km depths, for example by partial melting of underplated basalt (e.g. Petford & Gallagher, 2001) or release of silicic melts from a cumulate pile (e.g. Marsh, 2002), is precluded by Sr-isotope values that are elevated over mantle values in virtually all intermediate to silicic volcanic rocks in the TVZ. Available data on volatile contents in young felsic Taupo volcanics yield water contents of 4–6 wt % (e.g. Dunbar *et al.*, 1989*a*; Blake *et al.*, 1992; Dunbar & Kyle, 1993). Assuming that the magmas were water saturated (and neglecting CO_2), this corresponds to depths of ~5–8 km for the regions where crystallization and melt entrapment occurred. The age data here provide the first direct information about the country rocks that contribute to generation of the rhyolites between ~15 and ~5–8 km depth.

The U–Pb zircon model ages (Table 3) fall into two groups. The first group is inferred to be from plutonic sources younger than $0{\cdot}513 \pm 0{\cdot}112$ Ma and that reflect the onset of magmatism in this area. Ages from the 340 ka Whakamaru Ignimbrite (Brown & Fletcher, 1999) have a broadly similar cut-off at $0{\cdot}61 \pm 0{\cdot}02$ Ma. The absence of earlier Quaternary zircon ages in both datasets ($n = 54$) suggests that products of earlier TVZ silicic ignimbrites from 1·6 to 0·9 Ma (Houghton *et al.*, 1995) were not sourced in the area encompassed by the Whakamaru and Oruanui calderas (Fig. 1a). There is, however, no clear break between the Quaternary U–Pb dated zircons and the dominant populations of younger (U–Th dated) zircons, and hence no easy way from age data alone of having a universally applicable distinction between inherited and co-magmatic zircons.

The second age group is older than $91{\cdot}7 \pm 4{\cdot}1$ Ma and is inferred to represent zircons derived from late Palaeozoic to Mesozoic greywacke (meta-sandstones and -argillites) basement lithologies. These rocks contain heterogeneous populations of syn-sedimentation age and inherited zircons (Cawood *et al.*, 1999). Surface exposures of the greywackes around Taupo are grouped into the Torlesse and Waipapa terranes (e.g. Mortimer, 1994), with depositional ages of 170–160 and ~140 Ma, respectively. Our new zircon age data include three younger grains (Table 3), the ages of which are comparable with a sub-facies of the Torlesse, the Omaio petrofacies (Mortimer, 1994), which was deposited from ~112 to 95 Ma and contains a dominant population of zircons with similar model ages to the depositional age (Cawood *et al.*, 1999). The Omaio petrofacies, however, crops out at the surface ~200 km NNE of Taupo, and was not previously suspected to occur at depth beneath the TVZ. Thus an important implication of our data is that the age (and hence compositional) range of possible greywacke lithologies (or their high-grade equivalents) that could be melted to contribute to the genesis of TVZ rhyolites in general is wider than previously considered (e.g. Ewart & Stipp, 1968; Blattner & Reid, 1982; Conrad *et al.*, 1988; Graham *et al.*, 1992, 1995; Nicholls *et al.*, 1992; McCulloch *et al.*, 1994).

Generation of Taupo rhyolite magmas

Currently, the most favoured model for TVZ rhyolite genesis is by limited assimilation of greywacke by a mafic (mantle-derived) melt, followed by fractional crystallization (AFC; e.g. McCulloch *et al.*, 1994; Graham *et al.*, 1995). However, the presence of greywacke-derived zircons in magmas at Taupo implies that this pathway cannot apply to all of the rhyolites considered in this paper. To have old zircons in the rhyolites requires large-scale melting and disaggregation of their protolith, regardless of whether this is greywacke itself or a plutonic rock previously derived from a greywacke source. Evidence that the latter situation may occur is given by three zircon grains in Unit **Ω**, where ancient cores are overgrown by mid-Pleistocene rims (Table 3; Fig. 12a, c and e).

Calculations of zircon dissolution kinetics (above, and Table 4) suggest that the pre-Quaternary zircons had to have been incorporated into magmas that either were erupted rapidly enough (e.g. Unit **Ω**) or were sufficiently evolved (i.e. high Zr concentrations) so that old zircons were able to survive. We thus concur with Ewart & Stipp (1968) and suggest that a greater role may be envisaged for melting of greywacke protoliths in the genesis of Taupo rhyolites than has more recently been suggested.

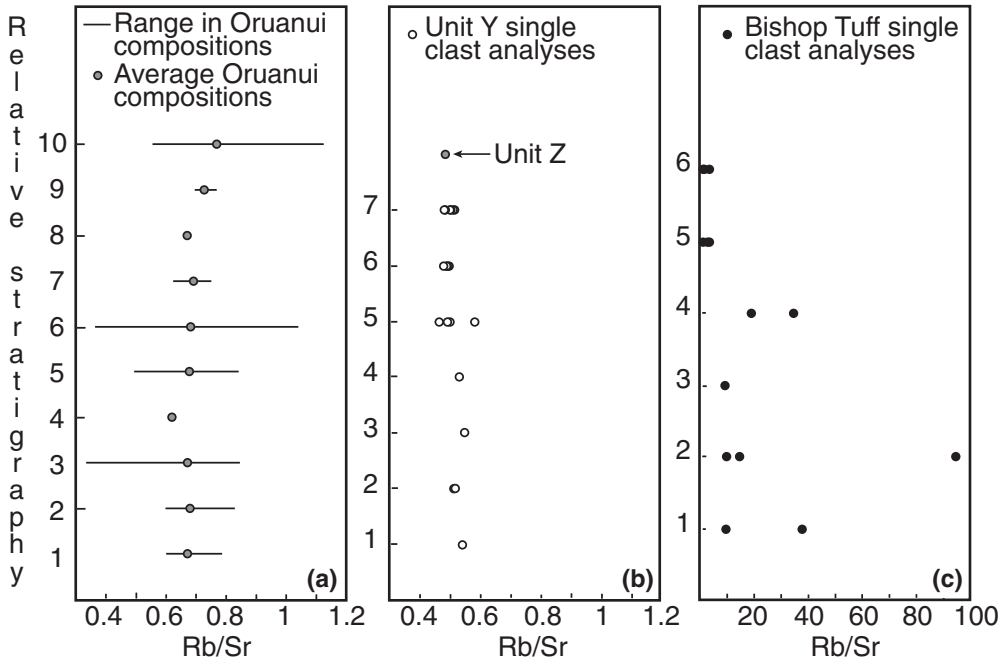

Fig. 20. Plot of Rb/Sr ratio vs relative stratigraphic height for (a) Oruanui, and (b) Units Y and Z [collectively the Taupo eruption of Wilson & Walker (1985)]. (c) Corresponding values for the Bishop Tuff [data from Hildreth (1979), stratigraphic order from Wilson & Hildreth (1997)], to show the extreme contrast in fractionation, and the lack of systematic zonation in the New Zealand examples.

Contradictions on the basis of isotopic data (e.g. Blattner & Reid, 1982; Graham *et al.*, 1992, 1995; McCulloch *et al.*, 1994) relate to specific samples from surficial greywacke domains in the Taupo area. However, our age data (Table 3) demonstrate that other greywacke domains are also present beneath Taupo.

Magmatic systems and magma chambers at Taupo

The zircon model-age spectra together with previously published data provide insights into what is meant by 'magmatic systems' at Taupo. In general, it is widely inferred (e.g. Hildreth, 1981) that within silicic magmatic systems there is present a source zone from which silicic magmas are generated and a chamber in which such melts accumulate and from which some proportion is erupted in any single event. At Taupo, the main 'source zone' is inferred to be a relatively shallow region ($\leq$15 km depth) from which silicic melts are generated by one or more mechanisms such as greywacke assimilation (see Ewart & Stipp, 1968) or AFC processes involving crustally contaminated and mantle-derived parental mafic melts (see McCulloch *et al.*, 1994; Graham *et al.*, 1995). Silicic melts, however generated, are inferred to rise and accumulate in magma chambers at shallower levels, and the nature and evolution of such magma chambers at Taupo is delineated from three lines of evidence.

First, for the most part there are no substantial variations in crystal content or chemistry in the rhyolite eruptives at Taupo, the main exceptions being within the Oruanui and between Unit D–Acacia Bay dome and bracketing eruptives (Sutton *et al.*, 1995, 2000; Wilson *et al.*, in preparation). In addition, the two largest eruptions (Oruanui and Unit Y) show no systematic zonation in composition with eruption order (Fig. 20). These data suggest that if there was a more crystal-rich root zone to the magma bodies evacuated in each eruption, then there were significant differences between the eruption products and any material that remained in the lower part of the chamber.

Second, the Unit S eruption involved an andesite magma ($\sim$59% SiO_2) that could, from the presence of hybrid rhyodacite generated along their mutual contact, be argued to have ponded below the otherwise unzoned, sparsely porphyritic (2–3 wt % crystals) rhyolite (Blake *et al.*, 1992). The density inferred for the andesite (2·43 g/cm^3; Blake *et al.*, 1992) is greater than that plausible for Unit S rhyolite with moderate amounts of crystals. It was thus inferred that the ponded andesite separated a crystal-poor rhyolite from an effectively solid floor (crystal-rich felsic mush or solid rock). Similarly, some mafic magma ponded below the Oruanui rhyolite for a short time period prior to evacuation (Wilson *et al.*, in preparation).

Third, the relationships between the zircon model-age spectra and abundances for the Tihoi, Okaia and Oruanui eruptions suggest that the magmas represented by our samples underwent a period of zircon crystallization in a body that was separate from the underlying material that is represented by the common model-age peak of

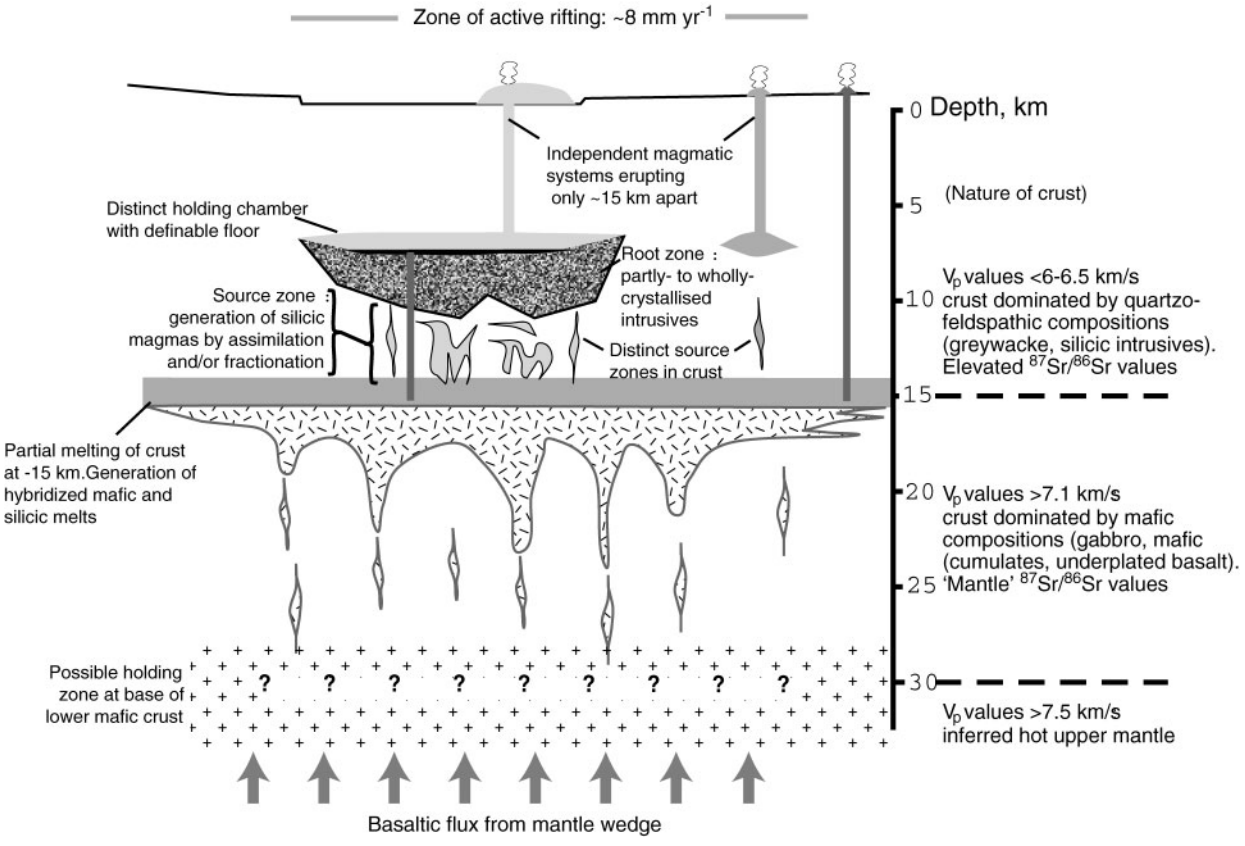

Fig. 21. Scaled schematic cross-section of the crust below Taupo volcano showing the inferred 2-D layout of the magmatic systems at ~25–30 ka. The ~15 km deep interface between a broadly 'quartzo-feldspathic' crust and denser material below is based on Stern & Davey (1987). M. Reyners (personal communication, 2003) supplied information on seismic velocities and the depth of the ~30 km deep interface between probable mafic crust and mantle. Significant amounts of zircon-bearing material are inferred to occur only above the ~15 km deep interface. The top(s) of the holding chamber(s) is/are inferred to be at 6–8 km minimum depth, based on volatile contents in glass inclusions (Dunbar *et al.*, 1989*a*; Y. Liu, personal communication, 2003) and phase equilibria (Ewart *et al.*, 1975; Blake *et al.*, 1992; Sutton *et al.*, 2000). (See text for discussion.)

~100 ka (Fig. 18). The underlying material is inferred to have been partly to wholly solidified mush to rock, from which part of the magma represented in each eruption was derived by some mechanism (remelting, liquid separation, etc.). This plutonic material, in broad terms temporally and compositionally related to crystal-rich dome-building activity just north of Lake Taupo (Whakaroa domes: Sutton *et al.*, 1995; Wilson *et al.*, in preparation) would thus largely be responsible for the overall similar compositional characteristics of the three magmas. The overlying magma body is envisaged to contain only the magma volume that was demonstrably erupted and not to have any significant zonation (Fig. 20; see Smith, 1979).

Thus at Taupo we suggest that the magmatic systems active over the past ~65 kyr have consisted of three entities: source zone, a root zone, and a holding chamber (Fig. 21).

The source zone is where the chemical and bulk isotopic characteristics of the magmas are created by complex processes of assimilation and fractionation, driven by inputs of mantle-derived mafic magmas, and modified by outputs of rhyolite magmas (and, rarely, modified mafic to intermediate magmas) upwards (Hildreth, 1981). Source zone temperatures are buffered by a large volume of rock and thus change gradually, as reflected in the rise in Fe–Ti oxide temperatures of the post-Oruanui rhyolitic eruptives at Taupo (Sutton *et al.*, 2000). Changes in chemistry and bulk isotopic attributes can, however, occur rapidly in either space or time, depending on the particular position where mafic magma inputs stall and assimilation of country rock takes place. Thus any contrasts between contemporaneously active but geographically distinct source zones (e.g. Rubbish Tip dome vs Okaia–Oruanui), and successively active but geographically overlapping source zones (such as those for the post-Oruanui rhyolite batches) are explained by changes in position of the thermal focus in the crust. Lithologies involved in the assimilation are inferred to be a mixture of greywacke (shown by zircon model ages in Units Ω and G), and plutonic rocks (including those of compositions evolved enough to have

preserved zircons through from a greywacke-age source) that were previously generated and largely to wholly crystallized. Other lithologies and other pathways to silicic compositions are possible, but these would neither preserve pre-existing zircon populations nor generate new zircon populations until zircon saturation had been reached (i.e. at ~70% SiO_2 in typical Taupo compositions).

Material representing the root zone to magma chambers below Taupo is inferred to largely be composed of partly crystallized mush to wholly crystallized plutonic material that is represented by the 'antecryst' zircons with model ages centred around 100 ka. Information is lacking to determine whether any of the pre-100 ka Quaternary plutonic or older greywacke-derived zircons may also have come from the root zone, or if they have been carried up from deeper levels. However, the model ages measured for the Oruanui common phases are inconsistent with the majority of these crystals being derived simply from stirring up and disaggregation of any root-zone mush.

The holding chamber corresponds to the erupted roofward portion of the magma chambers envisaged by Smith (1979) and Hildreth (1981), but at Taupo is inferred to have had a discrete lower boundary. Each chamber is envisaged by us as forming separately prior to, and being effectively emptied during, each eruption (or alternatively crystallizing to form a plutonic body in the absence of an eruption). Evidence for the holding chamber having a flat-lying discoidal shape is seen in the Unit S and Y eruptions (Blake *et al.*, 1992; Dunbar & Kyle, 1993). Most of the limited crystallization seen in the Taupo rhyolites is envisaged to have occurred during filling of, or in, the holding chamber, as reflected in the volatile saturation pressures of glass inclusions (Dunbar *et al.*, 1989*a*; Dunbar & Kyle, 1993) and the young average ages of common phases in the Oruanui and Unit Y.

Our model for the nature and development of magma chambers at Taupo is similar in some respects to that inferred for the climactic rhyodacite body at Crater Lake. In that case, an unzoned rhyodacite with 6–14% phenocrysts overlay a crystal-rich cumulate pile, with little sign of anything other than a sharp boundary between the two (Druitt & Bacon, 1989). The major contrast is in the overall mafic composition of the cumulate pile at Crater Lake, but its physical condition matches what we envisage for the top of the root zone to holding bodies at Taupo. U–Th model-age data from zircons in partially fused granodiorite blocks ejected in the climactic eruption (Bacon *et al.*, 2000) record the generation of a silicic plutonic body at ~110 ka and its partial remobilization prior to 7·7 ka. However, no data are available to indicate if these older zircons are present as antecrysts or xenocrysts (in the senses used here), in the 7·7 ka climactic ejecta. Growth of the ~100 ka antecryst zircon population at Taupo was contemporaneous with some dome-building and minor explosive activity.

In addition, we draw a distinction between average magma generation rates in the source zone and the rates at which that magma can be accumulated in the holding chamber prior to any eruption at Taupo. This distinction arises because of the possibility of generating bodies of eruptible magma by remobilization of hot, partly to wholly crystallized material in the root zone. If the surface geothermal flux is taken to reflect a long-term mantle-derived magma flux, then ~0·32 m^3/s of mafic magma is required to supply the geothermal heat flux around Taupo (Bibby *et al.*, 1995), and thus could generate of the order of 0·05–0·08 m^3/s of rhyolite by AFC processes (McCulloch *et al.*, 1994; Graham *et al.*, 1995). However, the average rhyolite eruption rate at Taupo over the past 65 kyr has been ~0·28 m^3/s, implying either that magma generation rates can be highly variable or that direct generation of significant amounts of rhyolite by remobilization or assimilation is occurring. In turn, accumulation rates in the holding chamber may be even higher. If the magma for the Okaia and Oruanui eruptions accumulated after the Tihoi eruption at ~45 ka, then the rate would have averaged 0·92 m^3/s. If the most extreme view is taken, on the basis of the similar abundances (Table 2) but differing model-age spectra (Fig. 18) of their zircon populations, that the Okaia and Oruanui came from separate holding bodies, the Oruanui magma accumulated in the time break between ~29 ka and ~26·5 ka, implying a rate of ~6·7 m^3/s. From other evidence, the third post-Oruanui rhyolite magma batch is inferred to have accumulated over ~600 years at a rate of ~1·9 m^3/s (Sutton *et al.*, 2000).

If the magma volume for any one eruption at Taupo approximates to the size of the holding chamber, then there need not be any direct relationship between the eruption size and repose period. The productivity of the overall magmatic system [source zone, accumulated plutonics and holding chamber(s)] can be estimated on the basis of the volume erupted divided by elapsed time, but the eruption timings and sizes may be controlled by non-systematic processes, including the mechanism of rhyolite generation and the volume of the holding chamber. Thus at Taupo (and elsewhere) although there may be a linear relationship between cumulative volume and cumulative time (Bacon, 1982; Froggatt, 1982), there is a chaotic relationship between the volume of any eruption and its preceding or following repose period (Wilson, 1993).

Implications of Taupo zircon age spectra for silicic magmatic systems

Phenocrysts vs antecrysts vs xenocrysts

In general, differences between the zircon ages recorded from silicic eruptives and the eruption age are interpreted

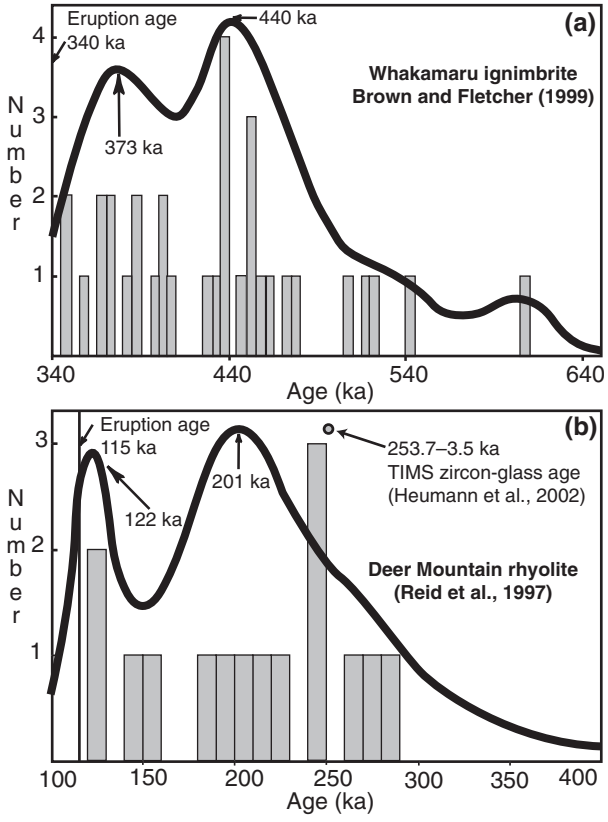

Fig. 22. (a) Histogram and PDF curve constructed from U–Pb zircon age data from the 340 ka Whakamaru Ignimbrite (Brown & Fletcher, 1999). (See text for discussion.) (b) Histogram and PDF curve based on zircon U–Th age data from Reid *et al.* (1997) to show the bimodality of the age distribution for the Deer Mountain dome at Long Valley, with the Heumann *et al.* (2002) bulk zircon-glass TIMS model age for comparison. (See text for discussion.)

to represent 'magma residence times' (e.g. Reid *et al.*, 1997; Brown & Fletcher, 1999; Reid & Coath, 2000; Vazquez & Reid, 2002). As such, the notion is held of variously 'longer' (e.g. Whakamaru Ignimbrite) or 'shorter' (e.g. Bishop Tuff) residence times, but our data suggest an alternative interpretation in some cases. For example, the Whakamaru model ages can be replotted (Fig. 22a) to show a bimodal distribution, the older mode of which could be interpreted, as in the younger Taupo cases, as being inherited. What then are the grounds for considering the 'magma residence times' of zircons at Taupo?

At Taupo, the zircon model ages range from <20 ka to >500 Ma. Clearly, many younger examples are phenocrysts that grew in the liquid in which they were frozen by eruption. Equally so, the Mesozoic- and Palaeozoic-aged grains are logically considered to be xenocrysts, incorporated by melting and disaggregation of their metasedimentary (although igneous-derived) host rocks. Between these two extremes, there is a significant proportion of the zircon crystal population of intermediate age, in particular the ~100 ka population peak in the Tihoi, Okaia and Oruanui eruptives (Fig. 18). Should such crystals be treated as phenocrysts or xenocrysts?

We interpret the ~100 ka zircon population to be derived from partly to wholly solidified plutonic bodies and, following Hildreth (presentation at Penrose Conference on 'Longevity and Dynamics of Rhyolitic Magma Systems', 2001), use the term 'antecryst' for such crystals, which are interpreted to predate the assembly of a magma body in the (holding) chamber from which it was erupted. The U–Th systematics of the Oruanui major phases (Fig. 7) show that the hornblende, magnetite and orthopyroxene crystals define an isochronous relationship with the whole rock that yields an age of 33 +18/−16 ka, consistent with these being dominantly phenocrysts as well. The plagioclase population contains minor proportions (1–5% of the >1 mm fraction) of crystals with grey cores that represent a non-phenocrystic population (Charlier *et al.*, 2003*a*). However, as the plagioclase separate falls on the equiline (Fig. 7), it is not certain on that basis whether the cores represent antecrysts or xenocrysts.

We thus consider 'magma residence times' at Taupo, i.e. the time periods over which bodies of moderately (Tihoi, Okaia, Oruanui) to sparsely porphyritic (post-Oruanui) rhyolites accumulated in the holding chamber from which they were erupted, to be exceptionally short. For the Oruanui, the maximum is ~40 kyr, represented by the period over which compositions of this type were erupted. The minimum is the ~2·5 kyr period between the Okaia and Oruanui eruptions. Zircons with Quaternary model ages older than ~60–70 ka are considered to have been recycled from partly to wholly solidified plutonics and not to record a true magma residence time as the host rocks were not eruptible. Previous work at Taupo had also suggested short magma residence times (hundreds to thousands of years) for the post-Oruanui succession on the basis of stepwise changes in geochemical characteristics (Sutton *et al.*, 1995, 2000), and these are consistent with the zircon model-age spectra.

The debate over magma residence times at large, young silicic systems elsewhere has focused around Long Valley, Yellowstone and Valles calderas. At Long Valley in particular, contrasting views have arisen over data from Rb–Sr, U–Th and U–Pb systematics, in terms of the residence time for the Bishop Tuff (Halliday *et al.*, 1989; Davies *et al.*, 1994; Davies & Halliday, 1998; Reid & Coath, 2000) and the contrasting residence times for small vs large eruptions (Reid *et al.*, 1997; Reid & Coath, 2000; Heumann *et al.*, 2002). Our data from Taupo suggest the following.

First, as proposed by Reid & Coath (2000), contrasts in model ages between U–Th and Rb–Sr systems at Long Valley imply that the former is the more reliable indicator of magma residence times in the holding chamber. At

Valles, Wolff & Ramos (2003) demonstrated that apparently coherent Rb–Sr isochrons are mixing lines, with no significance for magma residence times. The age spectra recorded by Rb–Sr systematics at Long Valley could thus be interpreted as complex functions of crystal remobilization, and a prolonged history of thermal waxing and waning of a source system (see Halliday, 1990; Mahood, 1990; Sparks *et al.*, 1990; Davies & Halliday, 1998). However, in contrast to the Oruanui, the Bishop Tuff holding chamber held a rhyolite body that was strongly zoned in crystal content and had undergone significant internal evolution (Fig. 20; Hildreth, 1979).

Second, in themselves the zircon model-age populations cannot be simply treated as directly representing magma residence times. For example, the Deer Mountain data of Reid *et al.* (1997, fig. 3) show a bimodality in the PDF (Fig. 22b), analogous to that seen in the Tihoi (Fig. 4c) and Okaia (Fig. 5c) eruptives. We suggest that an alternative interpretation of the Reid *et al.* (1997) data is that the older zircon populations in the Deer Mountain and South Deadman domes both represent antecrysts. We suggest that, in general, bimodality in zircon model-age spectra indicates remobilization of zircons from mush, rather than a prolonged evolutionary history in a continuously existing magma body. In contrast, the Bishop Tuff model-age spectrum is broadly unimodal (Reid & Coath, 2000) and, by analogy with the Rubbish Tip dome data (Fig. 6c), would therefore represent a true estimate of the residence time of magma in a continuous, mostly liquid body. Our explanation for bimodal (or multimodal) zircon model-age spectra would thus address the apparent conflict between apparently longer residence times for small eruptions at Long Valley (Reid *et al.*, 1997; Heumann *et al.*, 2002) than for the Bishop Tuff itself (Reid & Coath, 2000).

Nature of large silicic magmatic systems

In their generalized models of large silicic magmatic systems, Smith (1979) and Hildreth (1981) summarized conceptual frameworks within which most subsequent perceptions have been set. Our new data from Taupo, coupled with existing geochemical information, suggest some contrasts with these models that we highlight here.

There is evidence that the young rhyolites at Taupo were not systematically zoned with respect to composition or crystal content (Fig. 20). The most crystal-rich magmas were erupted in the Oruanui (6–13%), and the crystal contents of most post-Oruanui rhyolites are only 2–3·5 wt % (Sutton *et al.*, 2000; Wilson *et al.*, in preparation). No evidence has been found for compositions that might represent a more crystal-rich, denser, less-evolved root zone being systematically tapped in any eruption. Nor are the earliest eruptives noticeably crystal-poor: single clasts from the earliest material in the Oruanui eruption still contain 6–9 wt % crystals.

The notion that magma chambers were zoned structures was used, with other evidence, by Smith (1979) to suggest that in any eruption only ~10% of the volume of a magma chamber was likely to be erupted. The remaining 90% was considered to not erupt because of physical barriers, either of viscosity (e.g. as a result of elevated crystal contents) or of lower volatile content. At Taupo, such gradual limits seem not to have applied because, for example, of the lack of systematic variations in composition (Fig. 20), crystal contents or volatile abundances in the 1·8 ka Taupo (Unit Y) eruption, despite an extremely high climactic eruption rate (Wilson & Walker, 1985; Dunbar & Kyle, 1993; Sutton *et al.*, 1995). We infer there to have been a clear distinction between the rhyolites with their modest to low crystal contents erupted from a holding chamber and the material in the root zone that was left behind at depth. Although the thermal and chemical processes controlling the rhyolite volumes and compositions involve a large crustal volume, the actual volume of magma available to erupt is that which accumulates in the holding chamber. Thus in quiescent periods, there is possibly no large-scale magma body present, and the development of magma bodies during the lead-in to eruptions may be geologically rapid.

CONCLUSIONS

The zircon model-age data presented here confirm and strengthen previous inferences about the presence and rapid generation of different magma batches at Taupo (Sutton *et al.*, 1995, 2000). Prior to 26·5 ka, at least two independent, alternately active magma systems were present at Taupo, with vents only ~14 km apart. After the Oruanui eruption, subsequent magma batches represent three subtly different magma systems that were erupted sequentially from a restricted geographical area, largely overlapping with the Oruanui caldera outline, but showing independent chemical and isotopic characteristics. Zircon abundances and their consequent model-age spectra correlate with the degree of zircon saturation of the magmas. Undersaturated dacite yields a sparse suite of inherited zircons. Undersaturated to just-saturated rhyolites contain sparse mixed suites of inherited and newly grown grains. Oversaturated rhyolites contain abundant zircons with unimodal or bimodal model-age populations that are dominated by crystals still in U/Th isotopic disequilibrium.

The model-age spectra serve to divide zircons into phenocrysts, antecrysts and xenocrysts. Phenocrysts represent those crystals that formed in the magma body itself in the immediate build-up to the eruption. In the Oruanui, for example, zircon phenocrysts are all younger than ~60 ka and form the dominant population. Average model-age data from associated major phases in the

Oruanui imply that those are also mostly phenocrystic. Antecrysts are older crystals that were remobilized by remelting and disaggregation of their partly to wholly solidified host rocks. For example, the prominent peak of ~100 ka model ages in the pre-26·5 ka eruptives is interpreted to reflect zircon antecrysts from an earlier phase of rhyolite generation that correlates with modest-volume dome-building expression in surface volcanism. The model ages extend from ~100 ka with no clear break to 0·51 Ma (marking the onset of magmatism in this area), and then jump to ~92–527 Ma (i.e. the age range of grains or clasts in the local greywacke basement). Crystals from the latter suite of model ages are clearly xenocrysts, but no boundary can be defined between the ~100 ka suite of antecrysts and other <0·51 Ma possible xenocrysts.

The zircon model-age data also provide new perspectives on silicic magma generation at Taupo. Zircon xenocrysts provide direct evidence for some greywacke melting, but the age (and hence composition) of potential greywacke source rocks is greatly extended by our discovery of Cretaceous-aged zircons. Conclusions about the relative amounts of crystal fractionation from mantle-derived magmas (i.e. building new crust) vs assimilation processes (i.e. recycling existing crust) have now to be reassessed.

The time scales and associated rates for generation and eruption of silicic magmas at Taupo are unusually rapid. On a small scale, the presence of (euhedral) zircons in the Unit Ω dacite, in which composition they would dissolve within years to decades, implies that in that case a melting event and eruption were coincident within that timeframe. On a large scale, the overall production of rhyolite at Taupo over the past 65 kyr averages 0·28 m^3/s, whereas shorter-term accumulation rates for magma bodies that were evacuated in the Oruanui and Unit Y eruptions are inferred to have reached 0·43–6·7 m^3/s. Such accumulation rates are 1–2 orders of magnitude above those considered the norm for large silicic systems.

At Taupo we identify three crustal domains during the volcanism of the last ~65 kyr. The lowest (although ≤15 km deep) is the source zone, where the silicic magmas are generated, and where our age data support the inference of Ewart & Stipp (1968) that there is a direct role for melting of greywacke to generate silicic magmas. The middle domain is the root zone to the magma bodies, where melts accumulate and partly to wholly solidify, and from which the erupted compositions are extracted, in some examples carrying with them zircon antecrysts, most noticeably with an age population centred at ~100 ka. The upper domain, inferred to be at ~5–8 km depth, is the holding body in which most of the phenocryst population is crystallized, and from which the magmas are erupted. Based on the general lack of crystal content or chemical compositional gradients in the eruption products at Taupo, the holding body is inferred to have had a clear demarcation from the root zone (i.e. effectively to have had a 'floor'), and in most cases to have had a discoidal or sill-like morphology.

Our data serve also to highlight some questions related to silicic magmatism at Taupo and in general. First, if significant proportions of the zircons at Taupo are inherited antecrysts or xenocrysts [and there is evidence that this is the case with the plagioclase also (Charlier *et al.*, 2003*a*)], then what proportion of the major phases might be inherited? The average age of Oruanui major phases (Fig. 7) would suggest that they are all phenocrystic. However, the close similarity between the average ages of the Oruanui zircons and major phases implies that the multi-grain TIMS measurements cannot detect if a minority of the individual crystals are significantly older. Ideally, SIMS data from the major phases (or zircons included therein) could resolve how diverse the 'phenocryst' population is in these rhyolites. Parallel arguments could apply at Long Valley, Yellowstone and Valles calderas over the apparent ages obtained from different mineral species and consequent debate about the roles of inherited age and isotopic information (e.g. Christensen & DePaolo, 1993; Christensen & Halliday, 1996; Reid *et al.*, 1997; Davies & Halliday, 1998; Reid & Coath, 2000; Bindeman & Valley, 2001; Bindeman *et al.*, 2001; Heumann *et al.*, 2002; Wolff & Ramos, 2003).

Second, to what extent do bimodal or multimodal model-age distributions indicate the presence of inherited antecrystal or xenocrystal zircons? At Taupo, an important contrast is between the unimodal population present in the Rubbish Tip dome, and the mixed age populations of zircons present in the Oruanui magma and its precursor eruptions. In the former case a single magma generation and crystallization event is inferred, whereas in the latter zircons are in part inherited. We infer that the model-age spectrum in the Rubbish Tip dome zircons does represent a true 'magma residence time', but that in the Oruanui does not. From this we would suggest that of the zircon model-age spectra reported from Long Valley (Reid *et al.*, 1997; Reid & Coath, 2000), the unimodal spectrum for the Bishop Tuff may represent a true magma residence time, whereas the bimodal age distributions for some younger domes (Fig. 21b) do not. Instead, the Long Valley younger domes are interpreted by us to include remobilized antecrysts from earlier episodes of magmatism, and the zircon age spectrum cannot be used to support the notion of prolonged residence times.

Third, how can one define what is meant by the term 'magma chamber'? Should the crystals contained within immobile mush be counted as being resident in a magma chamber if the mush in itself is no longer capable of erupting unless remobilized by some new heat influx? Furthermore, does the term 'magma residence time'

have any meaning when referring to crystals in a mush, and if it does, how then might one distinguish at Taupo between crystals that have been contained in a still partly molten mush and the older Quaternary-aged zircons (back to 0·51 Ma) that must realistically have come from wholly crystallized bodies? At Taupo, even magma bodies as large as that which fed the Oruanui eruption appear not to be either systematically zoned or systematically tapped, in contrast to most documented examples worldwide.

ACKNOWLEDGEMENTS

We thank the following for financial support: UK NERC (grant NER/A/S/2000/01008; B.L.A.C. and J.P.D.), New Zealand Foundation for Research Science & Technology (C,J.N.W.), Royal Society of New Zealand Marsden Fund (C,J.N.W.) and The Open University (B.L.A.C.). Isotope research at The Open University is partly supported by NERC, and we thank Mabs Gilmour and Jo Rhodes for their assistance. We also thank Joe Wooden for his help, encouragement and advice in using the USGS–Stanford SHRIMP-RG. Discussions, critiques and assistance with this work from Wes Hildreth, Dan Morgan, Richard Price, Mark Reagan, Martin Reyners, Tom Sisson and Simon Turner are much appreciated. John Gamble is thanked for editorial handling. All ages were calculated using the Isoplot/Ex (v. 2.49) add-in for Microsoft Excel^{TM} by Ken Ludwig.

SUPPLEMENTARY DATA

Supplementary data for this paper are available at *Journal of Petrology* online.

REFERENCES

Annen, C. & Sparks, R. S. J. (2002). Effects of repetitive emplacement of basaltic intrusions on thermal evolution and melt generation in the crust. *Earth and Planetary Science Letters* **203**, 937–955.

Bacon, C. R. (1982). Time-predictable bimodal volcanism in the Coso Range, California. *Geology* **10**, 65–69.

Bacon, C. R., Persing, H. M., Wooden, J. L. & Ireland, T. R. (2000). Late Pleistocene granodiorite beneath Crater Lake caldera, Oregon, dated by ion microprobe. *Geology* **28**, 467–470.

Bergantz, G. W. (1989). Underplating and partial melting: implications for melt generation and extraction. *Science* **245**, 1093–1094.

Bibby, H. M., Caldwell, T. G., Davey, F. J. & Webb, T. H. (1995). Geophysical evidence on the structure of the Taupo Volcanic Zone and its hydrothermal circulation. *Journal of Volcanology and Geothermal Research* **68**, 29–58.

Bindeman, I. N. & Valley, J. W. (2001). Low-$\delta^{18}O$ rhyolites from Yellowstone: magmatic evolution based on zircons and individual phenocrysts. *Journal of Petrology* **42**, 1491–1517.

Bindeman, I. N., Valley, J. W., Wooden, J. L. & Persing, H. M. (2001). Post-caldera volcanism: in situ measurement of U–Pb age and oxygen isotope ratio in Pleistocene zircons from Yellowstone caldera. *Earth and Planetary Science Letters* **189**, 197–206.

Blake, S., Wilson, C. J. N., Smith, I. E. M. & Walker, G. P. L. (1992). Petrology and dynamics of the Waimihia mixed magma eruption, Taupo Volcano, New Zealand. *Journal of the Geological Society, London* **149**, 193–207.

Blattner, P. & Reid, F. (1982). The origin of lavas and ignimbrites of the Taupo Volcanic Zone, New Zealand, in the light of oxygen isotope data. *Geochimica et Cosmochimica Acta* **46**, 1417–1429.

Brown, S. J. A. & Fletcher, I. R. (1999). SHRIMP U–Pb dating of the preeruption growth history of zircons from the 340 ka Whakamaru Ignimbrite, New Zealand: evidence for >250 k.y. magma residence times. *Geology* **27**, 1035–1038.

Cawood, P. A., Nemchin, A. A., Leverenz, A., Saeed, A. & Ballance, P. F. (1999). U/Pb dating of detrital zircons: implications for the provenance record of Gondwana margin terranes. *Geological Society of America Bulletin* **111**, 1107–1119.

Charlier, B. L. A. (2000). U–Th isotopic constraints on the pre-eruptive dynamics of large-scale silicic volcanism: examples from New Zealand. Ph.D. thesis, The Open University, Milton Keynes.

Charlier, B. L. A. & Zellmer, G. F. (2000). Some remarks on U–Th mineral ages from igneous rocks with prolonged crystallisation histories. *Earth and Planetary Science Letters* **183**, 457–469.

Charlier, B. L. A., Davidson, J. P. & Wilson, C. J. N. (2003*a*). Generation processes in a high-silica rhyolite as recorded in plagioclase crystals from Taupo volcano, New Zealand. *Geophysical Research Abstracts* **5**, abstract 05352.

Charlier, B. L. A., Peate, D. W., Wilson, C. J. N., Lowenstern, J. B., Storey, M. & Brown, S. J. A. (2003*b*). Crystallisation ages in coeval silicic magma bodies: ^{238}U–^{230}Th disequilibrium evidence from the Rotoiti and Earthquake Flat eruption deposits, Taupo Volcanic Zone, New Zealand. *Earth and Planetary Science Letters* **206**, 441–457.

Christensen, J. N. & DePaolo, D. J. (1993). Time scales of large volume silicic magma systems: Sr isotopic systematics of phenocrysts and glass from the Bishop Tuff, Long Valley, California. *Contributions to Mineralogy and Petrology* **113**, 100–114.

Christensen, J. N. & Halliday, A. N. (1996). Rb–Sr ages and Nd isotopic compositions of melt inclusions from the Bishop Tuff and the generation of silicic magma. *Earth and Planetary Science Letters* **144**, 547–561.

Conrad, W. K., Nicholls, I. A. & Wall, V. J. (1988) Water-saturated and -undersaturated melting of metaluminous and peraluminous crustal compositions at 10 kb: evidence for the origin of silicic magmas in the Taupo Volcanic Zone, New Zealand and other occurrences. *Journal of Petrology* **29**, 765–803.

Dalrymple, G. B., Grove, M., Lovera, O. M., Harrison, T. M., Hulen, J. B. & Lanphere, M. A. (1999). Age and thermal history of the Geysers plutonic complex (felsite unit), Geysers geothermal field, California: a $^{40}Ar/^{39}Ar$ and U–Pb study. *Earth and Planetary Science Letters* **173**, 285–298.

Davies, G. R. & Halliday, A. N. (1998). Development of the Long Valley rhyolitic magma system: strontium and neodymium isotope evidence from glasses and individual phenocrysts. *Geochimica et Cosmochimica Acta* **62**, 3561–3574.

Davies, G. R., Halliday, A. N., Mahood, G. A. & Hall, C. M. (1994). Isotopic constraints on the production rates, crystallization histories and residence times of pre-caldera silicic magmas, Long Valley, California. *Earth and Planetary Science Letters* **125**, 17–37.

Druitt, T. H. & Bacon, C. R. (1989). Petrology of the zoned calkaline magma chamber of Mount Mazama, Crater Lake, Oregon. *Contributions to Mineralogy and Petrology* **101**, 245–259.

Dunbar, N. W. & Kyle, P. R. (1993). Lack of volatile gradient in the Taupo plinian–ignimbrite transition: evidence from melt inclusion analysis. *American Mineralogist* **78**, 177–184.

Dunbar, N. W., Hervig, R. L. & Kyle, P. R. (1989*a*). Determination of pre-eruptive H_2O, F and Cl contents of silicic magmas using melt inclusions: examples from Taupo volcanic centre, New Zealand. *Bulletin of Volcanology* **51**, 177–184.

Dunbar, N. W., Kyle, P. R. & Wilson, C. J. N. (1989*b*). Evidence for limited zonation in silicic magmatic systems, Taupo Volcanic Zone, New Zealand. *Geology* **17**, 234–236.

Ewart, A. & Stipp, J. J. (1968) Petrogenesis of the volcanic rocks of the central North Island, New Zealand, as indicated by a study of Sr^{87}/Sr^{86} ratios, and Sr, Rb, K, U and Th abundances. *Geochimica et Cosmochimica Acta* **32**, 699–735.

Ewart, A., Hildreth, W. & Carmichael, I. S. E. (1975). Quaternary acid magma in New Zealand. *Contributions to Mineralogy and Petrology* **51**, 1–27.

Froggatt, P. C. (1982). Review of methods for calculating the volume of rhyolite tephras—applications to the Taupo Volcanic Zone, New Zealand. *Journal of Volcanology and Geothermal Research* **14**, 301–318.

Ghiorso, M. S. & Sack, R. O. (1991). Fe–Ti oxide geothermometry: thermodynamic formulation and estimation of intensive variables in silicic magmas. *Contributions to Mineralogy and Petrology* **108**, 485–510.

Graham, I. J., Gulson, B. L., Hedenquist, J. W. & Mizon, K. (1992). Petrogenesis of late Cenozoic volcanic rocks from the Taupo Volcanic Zone, New Zealand, in the light of new lead isotope data. *Geochimica et Cosmochimica Acta* **56**, 2797–2819.

Graham, I. J., Cole, J. W., Briggs, R. M., Gamble, J. G. & Smith, I. E. M. (1995). Petrology and petrogenesis of volcanic rocks from the Taupo Volcanic Zone: a review. *Journal of Volcanology and Geothermal Research* **68**, 59–87.

Halliday, A. N. (1990). Reply to comment of R. S. J. Sparks, H. E. Huppert & C. J. N. Wilson on: 'Evidence for long residence times of rhyolitic magma in the Long Valley magmatic system: the isotopic record in precaldera lavas of Glass Mountain', by A. N. Halliday, G. A. Mahood, P. Holden, J. M. Metz, T. J. Dempster & J. P. Davidson. *Earth and Planetary Science Letters* **99**, 390–394.

Halliday, A. N., Fallick, A. E., Hutchinson, J. & Hildreth, W. (1984). A Nd, Sr and O isotopic investigation into the causes of chemical and isotopic zonation in the Bishop Tuff, California. *Earth and Planetary Science Letters* **68**, 379–391.

Halliday, A. N., Mahood, G. A., Holden, P., Metz, J. M., Dempster, T. J. & Davidson, J. P. (1989). Evidence for long residence times of rhyolitic magma in the Long Valley magmatic system: the isotopic record in precaldera lavas of Glass Mountain. *Earth and Planetary Science Letters* **94**, 274–290.

Hawkesworth, C. J., Turner, S. P., McDermott, F., Peate, D. W. & van Calsteren, P. (1997). U–Th isotopes in arc magmas: implications for element transfer from the subducted crust. *Science* **276**, 551–555.

Heumann, A., Davies, G. R. & Elliot, T. (2002). Crystallization history of the rhyolites at Long Valley, California, inferred from combined U-series and Rb–Sr isotope systematics. *Geochimica et Cosmochimica Acta* **66**, 1821–1837.

Hildreth, W. (1979). The Bishop Tuff: evidence for the origin of compositional zonation in silicic magma chambers. *Geological Society of America, Special Paper* **180**, 43–75.

Hildreth, W. (1981). Gradients in silicic magma chambers: implications for lithospheric magmatism. *Journal of Geophysical Research* **86**, 10153–10192.

Hildreth, W., Halliday, A. N. & Christiansen, R. L. (1991). Isotopic and geochemical evidence concerning the genesis and contamination of basaltic and rhyolitic magma beneath the Yellowstone Plateau volcanic field. *Journal of Petrology* **32**, 63–138.

Houghton, B. F., Wilson, C. J. N., McWilliams, M., Lanphere, M. A., Weaver, S. D., Briggs, R. M. & Pringle, M. S. (1995). Chronology and dynamics of a large silicic magmatic system: central Taupo Volcanic Zone, New Zealand. *Geology* **23**, 13–16.

Huppert, H. E. & Sparks, R. S. J. (1988*a*). The generation of granitic magmas by intrusion of basalt into continental crust. *Journal of Petrology* **29**, 599–624.

Huppert, H. E. & Sparks, R. S. J. (1988*b*). Melting the roof of a chamber containing a hot, turbulently convecting fluid. *Journal of Fluid Mechanics* **188**, 107–131.

Jellinek, A. M. & DePaolo, D. J. (2003). A model for the origin of large silicic magma chambers: precursors of caldera-forming eruptions. *Bulletin of Volcanology* **65**, 363–381.

Koyaguchi, T. & Kaneko, K. (1999). A two-stage thermal evolution model of magmas in continental crust. *Journal of Petrology* **40**, 241–254.

Lindsay, J. M., Williams, I. S., Ireland, T. R., Smith, I. E. M. & Black, P. M. (1994). Zircon ages in young felsic volcanics and underlying basement in northern New Zealand: implications for rhyolite genesis (abstract). *US Geological Survey Circular* **1107**, 196.

Lowenstern, J. B., Persing, H. M., Wooden, J. L., Lanphere, M. A., Donnelly-Nolan, J. & Grove, T. L. (2000). U–Th dating of single zircons from young granitoid xenoliths: new tools for understanding volcanic processes. *Earth and Planetary Science Letters* **183**, 291–302.

Ludwig, K. R. (2002). *Isoplot/Ex Version 2.49: a Geochronological Toolkit for Microsoft Excel*. Berkeley, CA: Berkeley Chronology Center.

Mahood, G. A. (1990). Second reply to comment of R. S. J. Sparks, H. E. Huppert & C. J. N. Wilson on: 'Evidence for long residence times of rhyolitic magma in the Long Valley magmatic system: the isotopic record in precaldera lavas of Glass Mountain', by A. N. Halliday, G. A. Mahood, P. Holden, J. M. Metz, T. J. Dempster & J. P. Davidson. *Earth and Planetary Science Letters* **99**, 395–399.

Marsh, B. D. (2002). On bimodal differentiation by solidification front instability in basaltic magmas, part 1: basic mechanics. *Geochimica et Cosmochimica Acta* **66**, 2211–2229.

McCulloch, M. T., Kyser, T. K., Woodhead, J. & Kinsley, L. (1994). Pb–Sr–Nd–O isotopic constraints on the origin of rhyolites from the Taupo Volcanic Zone of New Zealand: evidence for assimilation followed by fractionation from basalt. *Contributions to Mineralogy and Petrology* **115**, 303–312.

Mortimer, N. (1994). Origin of the Torlesse terrane and coeval rocks, North Island, New Zealand. *International Geology Review* **36**, 891–910.

Mungall, J. E. (2002). Empirical models relating viscosity and tracer diffusion in magmatic silicate melts. *Geochimica et Cosmochimica Acta* **66**, 125–143.

Newnham, R. M., Eden, D. N., Lowe, D. J. & Hendy, C. H. (2003). Rerewhakaaitu Tephra, a land–sea marker for the Last Termination in New Zealand, with implications for global climate change. *Quaternary Science Reviews* **22**, 289–308.

Nicholls, I. A., Oba, T. & Conrad, W. K. (1992). The nature of primary rhyolitic magmas involved in crustal evolution: evidence from an experimental study of cummingtonite-bearing rhyolites, Taupo Volcanic Zone, New Zealand. *Geochimica et Cosmochimica Acta* **56**, 955–962.

Paces, J. B. & Miller, J. D. (1993). U–Pb ages of Duluth complex and related mafic intrusions, northeastern Minnesota: geochronological insights to physical, petrogenetic, palaeomagnetic, and tectonomagmatic processes associated with the 1·1 Ga mid-continent rift system. *Journal of Geophysical Research* **98**, 13997–14013.

Palmer, K., Mortimer, N., Nathan, S., Isaac, M. J., Field, B. D., Sircombe, K. N., Black, P. M., Bush, S. & Orr, N. W. (1995). Chemical and petrographic analyses of some New Zealand

Paleozoic–Mesozoic metasedimentary and igneous rocks. *Lower Hutt, New Zealand: Institute of Geological & Nuclear Sciences, Science Report* **95/16**, 1–37.

Petford, N. & Gallagher, K. (2001). Partial melting of mafic (amphibolitic) lower crust by periodic influx of basaltic magma. *Earth and Planetary Science Letters* **193**, 483–499.

Reid, M. R. & Coath, C. D. (2000). In situ U–Pb ages of zircons from the Bishop Tuff: no evidence for long crystal residence times. *Geology* **28**, 443–446.

Reid, M. R., Coath, C. D., Harrison, T. M. & McKeegan, K. D. (1997). Prolonged residence times for the youngest rhyolites associated with Long Valley caldera: ^{230}Th–^{238}U ion microprobe dating of young zircons. *Earth and Planetary Science Letters* **150**, 27–39.

Schärer, U. (1984). The effect of initial ^{230}Th disequilibrium on young U–Pb ages: the Makalu case, Himalaya. *Earth and Planetary Science Letters* **67**, 191–204.

Shane, P. (1998). Correlation of rhyolitic pyroclastic eruptive units from the Taupo Volcanic Zone by Fe–Ti oxide compositional data. *Bulletin of Volcanology* **60**, 224–238.

Shaw, H. R. (1972). Viscosities of magmatic silicate liquids: an empirical method of prediction. *American Journal of Science* **272**, 870–893.

Shaw, H. R. (1985). Links between magma–tectonic rate balances, plutonism, and volcanism. *Journal of Geophysical Research* **90**, 11275–11288.

Smith, R. L. (1979). Ash-flow magmatism. *Geological Society of America, Special Paper* **180**, 5–27.

Sparks, R. S. J., Huppert, H. E. & Wilson, C. J. N. (1990). Comment on: 'Evidence for long residence times of rhyolitic magma in the Long Valley magmatic system: the isotopic record in precaldera lavas of Glass Mountain', by A. N. Halliday, G. A. Mahood, P. Holden, J. M. Metz, T. J. Dempster & J. P. Davidson. *Earth and Planetary Science Letters* **99**, 387–389.

Spera, F. J. & Crisp, J. A. (1981). Eruption volume, periodicity, and caldera area: relationships and inferences on development of compositional zonation in silicic magma chambers. *Journal of Volcanology and Geothermal Research* **11**, 169–187.

Stern, T. A. & Davey, F. J. (1987). A seismic investigation of the crustal and upper mantle structure within the Central Volcanic Region of New Zealand. *New Zealand Journal of Geology and Geophysics* **30**, 217–231.

Stockstill, K. R., Vogel, T. A. & Sisson, T. W. (2002) Origin and emplacement of the andesite of Burroughs Mountain, a zoned, large-volume lava flow at Mount Rainier, Washington, USA. *Journal of Volcanology and Geothermal Research* **119**, 275–296.

Sutton, A. N. (1995). Evolution of a large silicic magma system: Taupo volcanic centre, New Zealand. Ph.D. thesis, The Open University, Milton Keynes.

Sutton, A. N., Blake, S. & Wilson, C. J. N. (1995). An outline geochemistry of rhyolite eruptives from Taupo volcanic centre, New Zealand. *Journal of Volcanology and Geothermal Research* **68**, 153–175.

Sutton, A. N., Blake, S., Wilson, C. J. N. & Charlier, B. L. A. (2000). Late Quaternary evolution of a hyperactive rhyolite magmatic system: Taupo volcanic centre, New Zealand. *Journal of the Geological Society, London* **157**, 537–552.

Turner, S. P., Hawkesworth, C. J., van Calsteren, P. W., Heath, E., Macdonald, R. & Black, S. (1996) U-series isotopes and destructive plate margin magma genesis in the Lesser Antilles. *Earth and Planetary Science Letters* **142**, 191–207.

van Calsteren, P. W. & Schweiters, J.B. (1995). Performance of a thermal ionisation mass spectrometer with a deceleration lens system and post-deceleration detector system. *International Journal of Mass Spectrometry and Ion Processes* **146/147**, 119–129.

Vazquez, J. A. & Reid, M. R. (2002). Time scales of magma storage and differentiation of voluminous high-silica rhyolites at Yellowstone caldera, Wyoming. *Contributions to Mineralogy and Petrology* **144**, 274–285.

Vucetich, C. G. & Howorth, R. (1976). Late Pleistocene tephrostratigraphy in the Taupo District, New Zealand. *New Zealand Journal of Geology and Geophysics* **19**, 51–69.

Wark, D. A. (1991). Oligocene ash flow volcanism, northern Sierra Madre Occidental: role of mafic and intermediate-composition magmas in rhyolite genesis. *Journal of Geophysical Research* **96**, 13389–13411.

Watson, E. B. (1996). Dissolution, growth and survival of zircons during crustal fusion: kinetic principles, geological models and implications for isotopic inheritance. *Transactions of the Royal Society of Edinburgh: Earth Sciences* **87**, 43–56.

Watson, E. B. & Harrison, T. M. (1983). Zircon saturation revisited: temperature and composition effects in a variety of crustal magma types. *Earth and Planetary Science Letters* **64**, 295–304.

Wilson, C. J. N. (1993). Stratigraphy, chronology, styles and dynamics of late Quaternary eruptions from Taupo volcano, New Zealand. *Philosophical Transactions of the Royal Society of London, Series A* **343**, 205–306.

Wilson, C. J. N. (2001). The 26·5 ka Oruanui eruption, New Zealand: an introduction and overview. *Journal of Volcanology and Geothermal Research* **112**, 133–174.

Wilson, C. J. N. & Hildreth, W. (1997). The Bishop Tuff: new insights from eruptive stratigraphy. *Journal of Geology* **105**, 407–439.

Wilson, C. J. N. & Walker, G. P. L. (1985). The Taupo eruption, New Zealand. I. General aspects. *Philosophical Transactions of the Royal Society of London, Series A* **314**, 199–228.

Wilson, C. J. N., Houghton, B. F., McWilliams, M. O., Lanphere, M. A., Weaver, S. D. & Briggs, R. M. (1995). Volcanic and structural evolution of Taupo Volcanic Zone, New Zealand: a review. *Journal of Volcanology and Geothermal Research* **68**, 1–28.

Wilson, C. J. N., Charlier, B. L. A., Blake, S. & Sutton, A. N. (2002). Pyroclastic deposits from ca. 64 to 26·5 ka in the Maroa–Taupo area, New Zealand, reflect contemporaneous independent silicic magmatic systems. *EOS Transactions, American Geophysical Union* **83**(22), Western Pacific Geophysics Meeting Supplement, Abstract SE 51B-01.

Wolff, J. A. & Ramos, F. C. (2003). Pb isotope variations among Bandelier Tuff feldspars: no evidence for a long-lived silicic magma chamber. *Geology* **31**, 533–536.